PERGAMON

Deep-Sea Research II 48 (2001) 3107–3139

DEEP-SEA RESEARCH
PART II

www.elsevier.com/locate/dsr2

Distribution, composition and flux of particulate material over the European margin at 47°–50°N

I.N. McCave[a,*], I.R. Hall[a,1], A.N. Antia[b], L. Chou[c], F. Dehairs[d], R.S. Lampitt[e], L. Thomsen[f], T.C.E. van Weering[g], R. Wollast[c]

[a] *Department of Earth Sciences, University of Cambridge, Downing Street, Cambridge CB2 3EQ, UK*
[b] *Institut für Meereskunde, Universität Kiel, Düsternbrooker Weg 20, D-24105 Kiel, Germany*
[c] *Laboratoire d' Océanographie Chimique et Géochimie des Eaux, Université Libre de Bruxelles, Campus de la Plaine - CP 208, Boulevard du Triomphe, B-1050 Brussels, Belgium*
[d] *Dienst Analytische Scheikunde, Vrije Universiteit Brussel, Pleinlaan 2, B-1050 Brussels, Belgium*
[e] *Southampton Oceanography Centre, Empress Dock, Southampton SO14 3ZH, UK*
[f] *GEOMAR, Wischhofstrasse 1-3, D-24148 Kiel, Germany*
[g] *Netherlands Institute for Sea Research (NIOZ), P.O. Box 59, 1790 AB Den Burg, Texel, The Netherlands*

Abstract

In the framework of the Ocean Margin Exchange project, a multi-disciplinary study has been conducted at the shelf edge and slope of the Goban Spur in order to determine the spatial distribution, quantity and quality of particle flux, and delineate the transport mechanisms of the major organic and inorganic components. We present here a synthesis view of the major transport modes of both biogenic and lithogenic material being delivered to the open slope of the Goban Spur. We attempt to differentiate between the direct biogenic flux from the surface mixed layer and the advective component, both biogenic and lithogenic.

Long-term moorings, instrumented with sediment traps, current meters and transmissometers have yielded samples and near-continuous recordings of hydrographic variables (current direction and speed, temperature and salinity) and light transmission for a period of 2.5 years. Numerous stations have been occupied for CTD casts with light transmission and collection of water samples. The sedimenting material has been analysed for a variety of marker compounds including phytoplankton pigments, isotopic, biomineral and trace metal composition and microscopical analyses. These samples are augmented by seasonal information on the distribution and composition of fine particles and marine snow in the water column.

The slope shows well-developed bottom nepheloid layers always present and intermediate nepheloid layers intermittently present. Concentrations are mainly in the range 50–130 mg m^{-3} in nepheloid layers and 6–25 mg m^{-3} in clear water. A seasonal variability in the concentration at the clear water minimum is

*Corresponding author. Fax: +44-1233-333-450.
E-mail address: mccave@esc.cam.ac.uk (I.N. McCave).
[1] Department of Earth Sciences, Cardiff University, Park Place, Cardiff CF10 3YE, UK

PII: S0967-0645(01)00034-0

argued to be related to seasonal variations in vertical flux and aggregate break-up in transit during summer months. It is suggested that the winter sink for this seasonal change in particulate matter involves some re-aggregation and scavenging, and some conversion of particulate to dissolved organic matter. This may provide a slow seasonal pump of dissolved organic carbon to the deep ocean interior. Differences in trapped quantities at different water depths are interpreted as due to lateral flux from the continental margin. There is a major lateral input between 600 and 1050 m at an inner station and between 600 and 1440 m at an outer one. The transport is thought to be related to intermediate nepheloid layers, but those measured are too dilute to be able to supply the flux. Observed bottom nepheloid layers are highly concentrated very close to the bed (up to $5\,g\,m^{-3}$), with a population of large aggregates. Some of these are capable of delivering the flux seen offshore during intermittent detachment of nepheloid layers into mid-water. Concentrated bottom nepheloid layers are also able to deliver large particles with unstable phytoplankton pigments to the deep sea floor in a few tens of days. Calculated $CaCO_3$ fluxes are adjusted for dissolution, which is inferred from Ca/Al ratios to be occurring in the $CaCO_3$-saturated upper water column where up to 80% of the $CaCO_3$ resulting from primary production is dissolved.

1. Introduction

The Ocean Margin Exchange (OMEX) project included several studies dealing with the distribution in the water column of particles, their composition and flux. As a work of synthesis this paper is dependent on the individual studies of contributors to the project and is clearly not able to include all the underpinning data, but contains enough to show the main features of particle fields.

Ever since Walsh et al. (1981) indicated that continental shelves and slopes might function as a significant sink for atmospheric CO_2, several studies have been specifically designed to examine shelf edge exchange processes, most notably in the Mid-Atlantic Bight on the eastern US continental shelf and slope during SEEP-I and SEEP-II (Walsh et al., 1988; Biscaye et al., 1994; Churchill et al., 1988), ECOMARGE in the Gulf of Lions (Monaco et al., 1990) and detailed studies on the continental slope off Cape Hatteras (Blake and Diaz, 1994).

During SEEP-I Biscaye et al. (1988) found that local grazing, sedimentation, decay, and shallow along-shelf transport limited the annual carbon export to less than 10% of shelf production. Similarly, during SEEP-II, further to the south off Cape Hatteras, Biscaye et al. (1994) suggest only a small proportion ($\ll 5\%$) of the biogenic particulate matter was exported to the adjacent continental slope and much of it may have been deposited originally on the shelf or shelf break and then resuspended and transported down slope thousands of years later (Anderson et al., 1994).

The importance of canyon-fed transport was noted in ECOMARGE, based in the Gulf of Lions, with export of material preferentially occurring down the canyon systems, notably the Lacaze-Duthiers Canyon (Monaco et al., 1990). The role of canyons also was examined by Gardner (1989a, b), who observed intermittent resuspension by internal waves and flux of sediment out of Baltimore Canyon in intermediate nepheloid layers (INLs).

A number of studies of sediment dispersal from the shelf have noted the presence of INLs off the continental slope (Drake, 1971, 1974; Baker and Hickey, 1986; Dickson and McCave, 1986; Thorpe and White, 1988; Monaco et al., 1990; Durrieu de Madron et al., 1990, 1993; Ruch et al.,

1993). Dickson and McCave (1986) and Thorpe and White (1988) showed many such layers on the west side of the Porcupine Bank just to the north of the present study area, suggesting they result from generation of a concentrated bottom nepheloid layer (BNL) by intensification of the internal tide and its detachment and spreading along isopycnal surfaces.

Our objective here is to define the concentration field of particulate material (PM) and aspects of its composition and variability. We then look at implications for fluxes through interaction with the current field and also consider the vertical settling flux measured in traps.

The observations on which the study is based were made from six ships (total of 10 cruises) and three moorings in the period May 1993–October 1995 over the bathymetric feature called Goban Spur. This feature has relatively smooth topography extending westwards from the Celtic Sea between 48° and 50°N but with two steeper scarps towards the base of the slope below 3000 m (Fig. 1). It is bounded to the south-east by rugged topography deeply incised by canyons, to the north by the large embayment of Porcupine Sea Bight. The adjacent continental shelf of the Celtic Sea is sandy and well known for tidal currents and sand ridges formed at low sea level stand

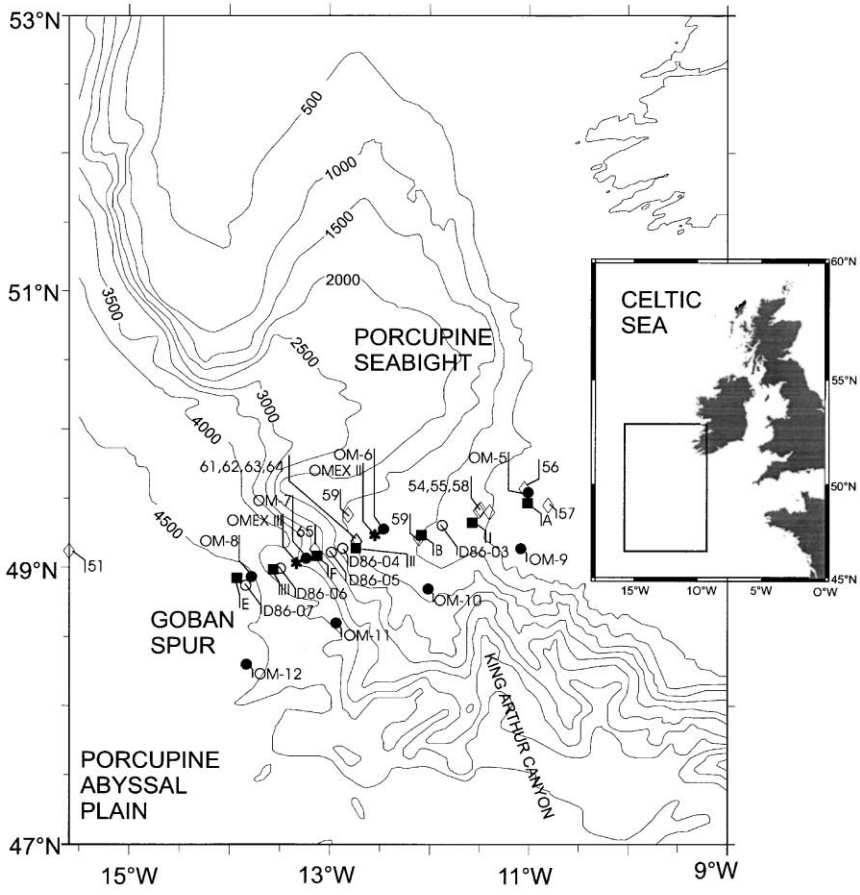

Fig. 1. Bathymetric chart of the Goban Spur area with stations for which data are referred to in the text: CTD, filled circles; large particle camera, open diamonds; traps, star; boundary layer, filled squares; filtered samples, open circles.

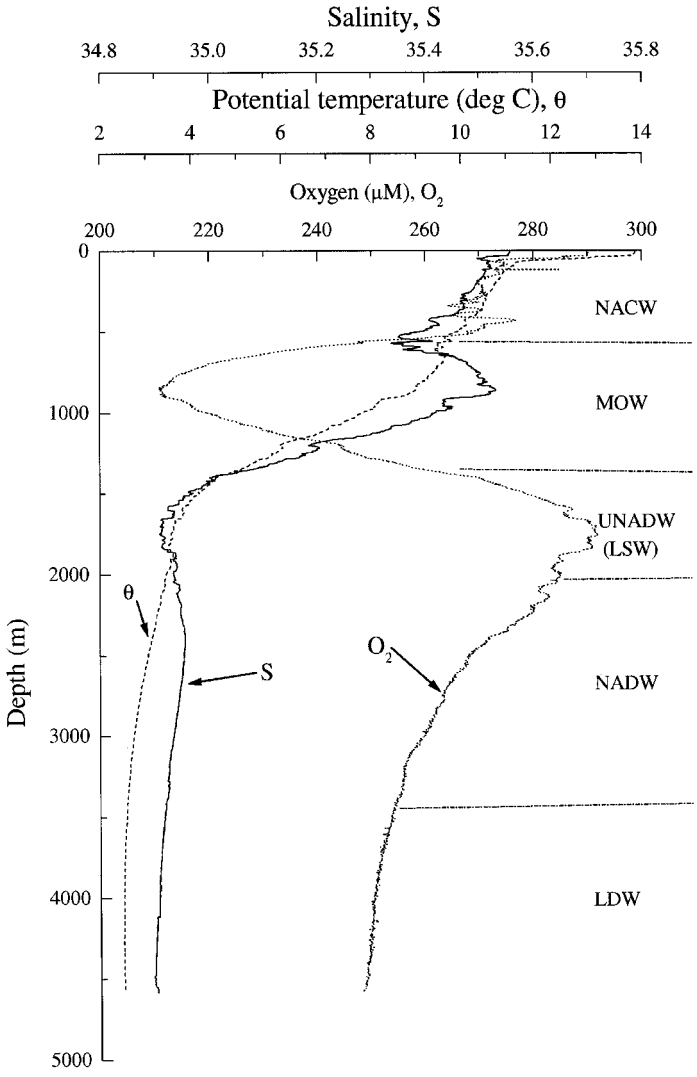

Fig. 2. Hydrographic parameters showing water masses at the outer Goban Spur. NACW: North Atlantic central water, MOW: Mediterranean outflow water, LSW: Labrador sea water, UNADW: upper North Atlantic deep water, LDW: lower deep water (for θ-S definitions see Harvey, 1982; McCartney, 1992).

(Hamilton et al., 1980; Belderson et al., 1986). Along the canyoned part of the slope, the shelf sand transport vectors go directly to the shelf edge (Johnson et al., 1982). This probably explains the origin of the canyons via erosive sandy turbidity currents.

The slope shallower than about 1000 m is swept by a poleward flowing slope current (Huthnance, 1995; Pingree and Le Cann, 1989), which contains North Atlantic central water (NACW) formed in the NE Atlantic by deep wintertime convection (Harvey, 1982) and the low oxygen signature of Mediterranean outflow water (MOW) in its lower part (Fig. 2). Below that is high oxygen-low salinity Labrador sea water (LSW) and other components of North Atlantic

deep water (NADW), and at the base of the slope is the northward flowing lower deep water (LDW) of McCartney (1992) with characteristic elevated silicate values ($\geqslant 35\,\mu M$) below 3000 m (Fig. 2) (Vangriesheim and Khripounoff, 1991). Bottom sediments are calcareous muds with carbonate increasing from about 40% at the top of the slope to 70% at its base. Sand content declines downslope from 90% to $<10\%$, but also changes from quartz to carbonate (foraminifera) (van Weering et al., 1998).

2. Methods

2.1. Transmissometry and nephelometry

A total of 116 CTD stations providing detailed hydrographic data on temperature, salinity, oxygen, fluorescence, transmission and scattering (but not all parameters on all casts) were obtained during three cruises: R.R.S. *Charles Darwin* cruises 84 (*CD84*; 18 January–2 February, 1994) and 94 (*CD94*; 3–20 June, 1995) and R.R.S. *Discovery* cruise 216 (*D216*; 26 August–12 September, 1995) providing satisfactory spatial and temporal coverage (Fig. 1). Optical attenuation measurements were made with a 0.25 m-path-length SeaTech transmissometer. There is substantial literature relating to the SeaTech instrument and its performance in nepheloid layers (Bartz et al., 1978; McCave, 1983; Spinrad et al., 1983; Gardner et al., 1985; Bishop, 1986). During *CD84* light scattering also was determined with a Chelsea Instruments Aquatraka MkII nephelometer. This instrument measures scattered violet (430 nm) light at 90° to the axis of the beam, a relatively insensitive region of the angular distribution of scattered light. In addition, the light wavelength is not optimal for detection of terrigenous particles. Nevertheless, the instrument has proven to be satisfactorily sensitive by comparison with the transmissometer, though it is more sensitive to the smaller particles in the size spectrum (Zaneveld, 1974; McCave, 1986).

Water was filtered to determine the mass concentration of PM gravimetrically, and to examine the composition of filtered particles using scanning electron microscopy. Usually 20 l samples were taken, filtered and weighed using standard high precision methods (0.4 μm pore polycarbonate membranes, laminar flow hood handling, 10^{-6} g balance with static reduction).

As the size, shape and refractive index of the material in the water column vary from place to place, a single literature equation cannot be used to relate attenuation to suspended matter concentration (McCave, 1983; Baker and Lavelle, 1984; Gardner et al., 1985; Moody et al., 1986; Gardner, 1989a). Our calibration is based on samples taken in layers of high optical turbidity (INLs and BNLs) and intervening clear waters and is expressed as $C_c = 977c - 357$ (with $n = 35$; $r = 0.95$), where C_c = PM concentration in mg m^{-3}; c = attenuation coefficient in m^{-1} (This equation is inverted from the regression of c on C). Pure (particle-free) sea water has a transmission of 91.3% per 0.25 m at 660 nm, corresponding to an attenuation coefficient of $c_w = 0.364$ according to the manufacturers. The intercept of c versus PM gives a value for c_w of 0.358 for zero PM according to Bishop's (1986) determination for seawater in situ. The zero-intercept value of c_w of 0.365 in our calibration is satisfactorily close. A calibration similar to the above for the Aquatraka nephelometer used during cruise *CD84* gives the relationship between the nephelometer voltage and PM concentration as $C_n = 467N - 1530$ (with $n = 13$; $r = 0.73$), where C_n = PM concentration in mg m^{-3}, N = Nephelometer output voltage on a 0–5 V scale.

2.2. Particle camera

It has become increasingly clear over the past 25 years that large particles, which are not satisfactorily sensed by optical methods or collected by water bottles, play a key role in marine particle dynamics (McCave, 1975). We used two optical sensing and counting systems for determining concentrations of large particles in (a) the water column (Lampitt et al., 1993a) and (b) the bottom boundary layer (Thomsen et al., 1994).

Marine snow particles are often extremely fragile (Alldredge and Gotschalk, 1988) and therefore require non-invasive in situ techniques to measure them. An underwater 35 mm still camera photographed a volume of water defined by an orthogonal collimated beam from a strobe light. The volume illuminated and visible by the camera is 40 l although only a portion of this is used for the analysis. Up to 400 frames are taken during any one deployment firing every 15 or 30 s (Lampitt et al., 1993a). Analysis of the images was carried out using a Kontron Bidas system. The negative of each frame is imported using a high-definition charged coupled device camera. The maximum and minimum dimensions of each particle are measured from which a volume is calculated and the equivalent spherical diameter (ESD) determined. Particles are attributed to one of six logarithmic size classes on the basis of their ESD, and the abundance and volume concentration within each of these classes is determined. Profiles were taken in the region of the Goban Spur on 67 occasions during five cruises to provide good seasonal and spatial coverage on the abundance, volume concentration, and size distribution of marine snow aggregates.

An important next step was to estimate the mass of material contained within these aggregates so that a comparison could be made with distribution of particles determined from transmissometer profiles and flux of material determined by sediment traps. Using published estimates of the density of large amorphous aggregates (McCave, 1984; Alldredge and Gotschalk, 1988), dry mass concentration was derived from volume concentration. These two relationships are somewhat different, giving higher values with the empirically determined relationship of Alldredge and Gotschalk.

2.3. Boundary layer sampling

Bottom water was sampled with the BIOPROBE system (Thomsen et al., 1994). The sampler consists of a system, which sucks discrete water samples through nozzles at 0.05, 0.10, 0.20 and 0.40 m above the sea bottom (m.a.b.). Videopictures of aggregates at 0.20, 0.40 and 5.0 m.a.b. were recorded with the particle camera. Flow speed in the bottom boundary layer (BBL) was measured with a thermistor flow meter at 0.30 m.a.b. and with particle cameras (Thomsen and Ritzrau, 1996). Turbidity in the BBL was measured with optical backscatter sensors or a 0.25 m pathlength SeaTech transmissometer. A normal deployment of BIOPROBE involved lowering the instrument system to the sea floor using a single-conductor cable. BIOPROBE typically came to rest with its feet having penetrated the sediment to a depth of 1–4 cm. A period of 6 min was maintained before sampling to allow material resuspended during deployment to drift away with the current. During the R.V. *Pelagia* cruise in August 1995, two aggregate cameras were attached to BIOPROBE to determine the sizes of resuspended sediments and the horizontal aggregate flux ($>100\,\mu m$) at 0.20 and 0.40 m.a.b. (Thomsen and Ritzrau, 1996).

Settling velocities of fresh phytodetritus and fluff (sediment/phytodetritus mixture) sucked up by BIOPROBE from the study site were determined in the cool-lab with a settling cylinder under in situ temperature conditions. The sizes of the disaggregated particles, sampled in the BBL with BIOPROBE were measured with a Coulter Counter.

2.4. Chemical measurements

The particulate organic carbon content (POC) of the water was measured on samples filtered onto precombusted GF/F filters (nominally 0.7 μm particle retention) with a Heraeus CHN-Analyser using methods of von Bodungen et al. (1991). A full description of the trap methodologies is given in Antia et al. (1999). Trap material was analysed by Wollast and Chou (1998) using ICP emission spectroscopy on totally digested samples for Al, Si and Ca after extraction with acetic acid. POC was determined by HT combustion on acidified samples by Antia et al. (1999). Ca was used to estimate $CaCO_3$ and Al to obtain the lithogenic fraction assuming it to be 7% of that material (Martin and Whitfield, 1983).

3. Particulate matter distributions

3.1. Distribution of fine particles

3.1.1. Winter conditions

Profiles obtained during *CD84* display several nepheloid layers (Fig. 3). A distinct surface nepheloid layer (SNL) whose thickness in deeper stations (OM-7 and OM-8), at around 300 m, is comparable with that of the mixed layer, is well marked in transmissometer but weak in nephelometer records, generally decreases in intensity off shelf, to concentrations of $\sim 50\,mg\,m^{-3}$. At the Sediment Transport And Boundary Layer Equipment (STABLE) and OM-6 stations, transmissometer and nephelometer profiles merge close to the base of the mixed layer. Further offshore at stations OM-7 and OM-8 the profiles merge at a greater depth of around 1000 m. The differences are most likely caused by the different sensitivities of each instrument to particle size (nephelometer greater to finer sizes (Zaneveld, 1974; McCave, 1986)), and suggest that coarser particles are more abundant in the SNL. Dickson and McCave (1986) found a distinct coarser particle size peak of probable biological origin within the SNL just north of here.

At stations OM-5, STABLE and OM-6 near-bottom values show a BNL extending about 150 m.a.b. (~ 1020 m; on density surface $\sigma_t = 27.63$), with peak suspended sediment concentrations at stations STABLE and OM-6 of $\sim 60\,mg\,m^{-3}$ based on transmission. Concentrations based on nephelometry are $> 100\,mg\,m^{-3}$ at 5–10 m.a.b. (1183 m; $\sigma_t = 27.68$). Material eroded from the bottom is liable to stay in the water column for a substantially longer duration than the high stress event leading to its initial resuspension (Gross and Nowell, 1990). The persistent bottom current with a northward flowing residual but also high-speed downslope excursions (Dickson et al., 1985; Pingree and Le Cann, 1989; Huthnance, 1995; van Weering et al., 1998; Pingree et al., 1999) will transport fine particles towards the north but resuspend large aggregates and move them downslope. Float data show strong transport basinward on isopycnal surfaces

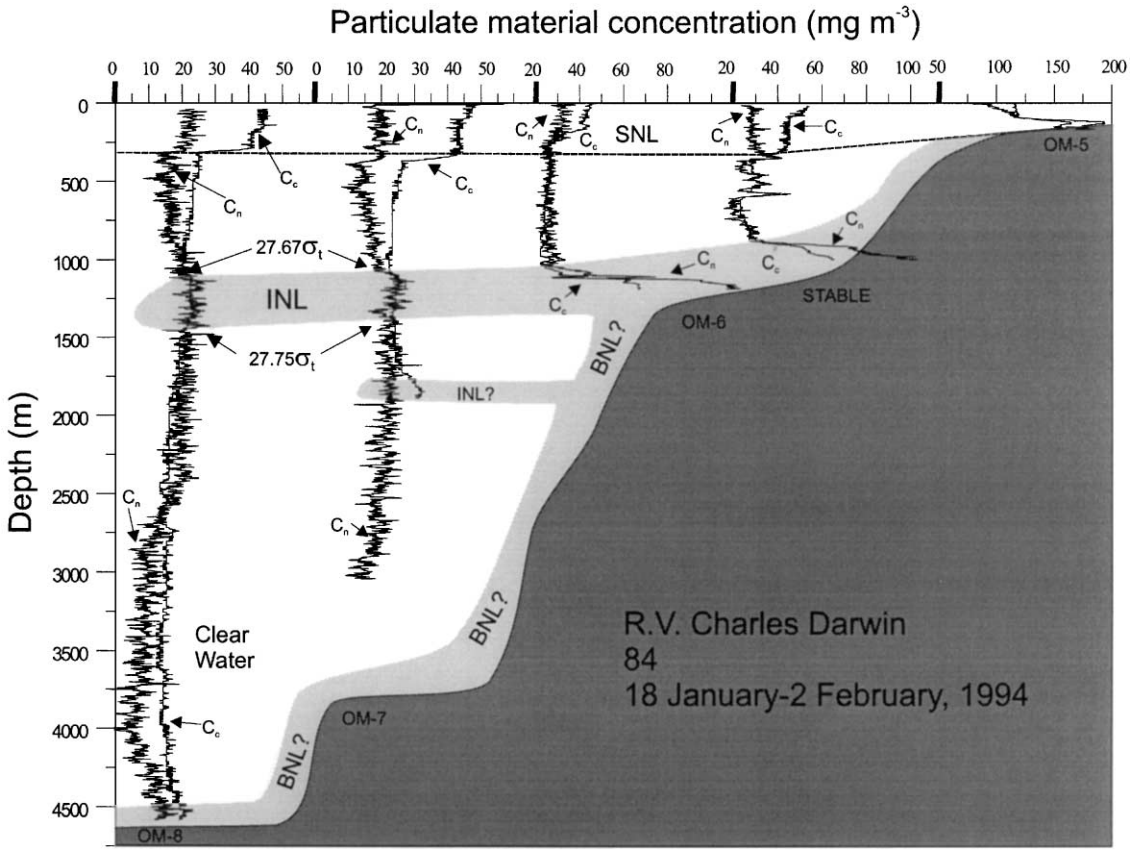

Fig. 3. Turbidity distribution with depth over Goban Spur sediment trap transect during *CD84* (Winter). Estimates (C_c, C_n) based on transmission and nephelometry profiles.

(see below). At the deepest station (OM-8) the intensity of the BNL is weak, suggesting low current activity.

At the STABLE station a series of INLs are present, between $\sim$400 and 600 m. The structure and intensity is coherent between the transmissometer and nephelometer profiles. These features do not appear at station OM-6 some 90 km to the west. A distinct, albeit weak, INL is also present at stations OM-7 and OM-8, with the top of the INL (defined by transmission) at $\sim$1080 m ($\sigma_t = 27.67$) and its base at $\sim$1250 m ($\sigma_t = 27.72$) at station OM-7; density surfaces almost coincident with the limits of the BNL seen at OM-6. Further offshelf, at station OM-8, the base of the INL has extended down to $\sim$1550 m ($\sigma_t = 27.75$). The sediment concentration over much of the interval in both profiles is $\sim 25\,\mathrm{mg\,m^{-3}}$, a small increase relative to the clear water minimum of $\sim 15\,\mathrm{mg\,m^{-3}}$.

As previously noted by Gardner et al. (1985) the transmissometer-based clear water minimum ($C_{\mathrm{min(c)}}$) of $\sim 10\,\mathrm{mg\,m^{-3}}$ occurs at a shallower depth than the nephelometer-clear water $C_{\mathrm{min(n)}}$, a feature present here also (station OM-8, Fig. 3). Gardner et al. (1985) were not able to determine

whether this difference was due to a response to different particle properties, or an effect of pressure or temperature on one or both instruments. We used a different nephelometer, but the range of possibilities is still too large for us to eliminate any.

3.1.2. Summer conditions

Similar features are seen in summer but with the notable exception of a lack of offshore INLs (Figs. 4 and 5). Concentrations in the SNL are substantially higher than in winter, (460 mg m^{-3} at OM-5), and decrease steadily off shelf to 250 mg m^{-3} by OM-8. The mixed layer is not evident and particle concentration at the deeper station remains generally high down to around 1000 m. The BNL is well developed at all stations, but concentrations decrease with increasing station depth, concentrations 10 m.a.b. at OM-5 and OM-8 being $\sim$120 and 43 mg m^{-3}, respectively. The vertical extent of the BNL (with respect to $C_{\min(c)}$) increases with depth from $\sim$125 m thick at station OM-5 to $\sim$450 m at OM-8 (this justifies the decision to put sediment traps no closer than 400 m.a.b., see below).

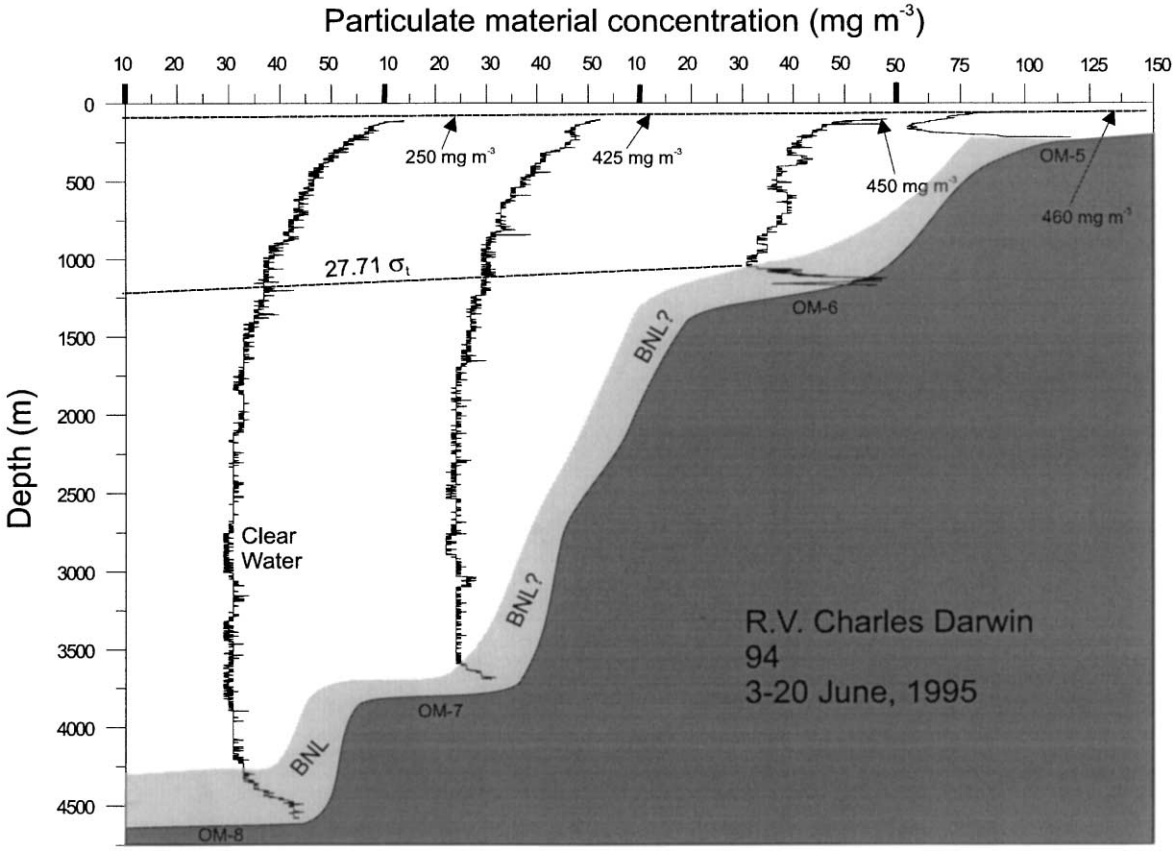

Fig. 4. Turbidity distribution (based on transmission) with depth over Goban Spur sediment trap transect during *CD94* (Summer). Data shallower than 100 m are not shown so as to allow a scale which reveals the structure of the deep water.

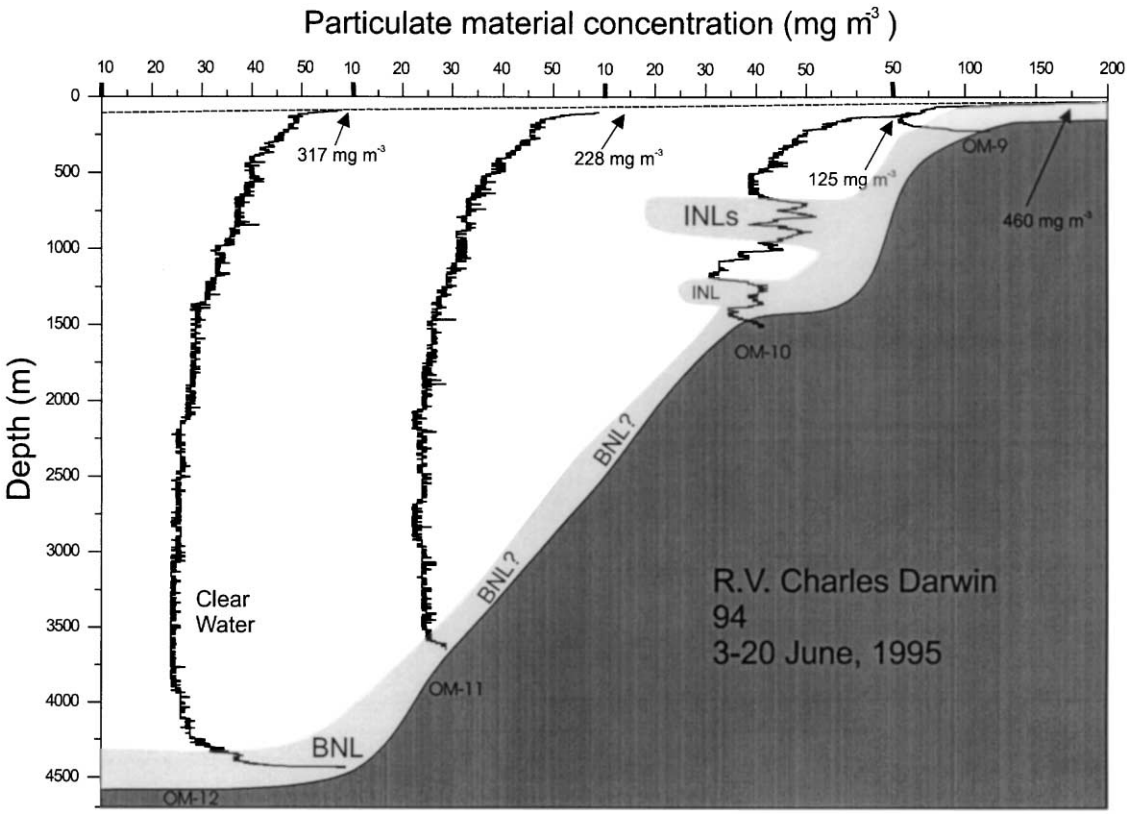

Fig. 5. Turbidity distribution (based on transmission) with depth over Goban Spur southern transect during *CD94* (Summer). Data shallower than 100 m are not shown so as to allow a scale which reveals the structure of the deep water.

A strong INL (51 mg m^{-3}) is seen at station OM-10 on a transect 55 km to the south (Fig. 5), and a weaker INL (40 mg m^{-3}) at station OM-6 (Fig. 4), both with a top at around 600 m ($\sigma_t = 27.34$). This feature is not present in the deep station profiles, demonstrating the spatial/temporal intermittency of INLs.

The summer $C_{\min(c)}$ at the deeper stations OM-7 and OM-8 was between 25 and 30 mg m^{-3}, approximately double the winter level. We do not believe this is due to a transmissometer offset because the calibration data are tight ($r = 0.95$) and comprise data from both winter and summer, with the correct zero intercept mentioned above. In addition the long-term transmissometer set at 1050 m depth at OMEX station II by Antia et al. (1999) shows a slight excursion in the attenuation coefficient, rising from 0.365 to 0.372 and back again between April and September 1994. This is equivalent to a concentration increase of 7 mg m^{-3} in summer. These values for the summer $C_{\min(c)}$ are thus highly reasonable given the five-to-ten fold increase in surface concentration, driven by spring and summer production. Somehow the summer clear water concentration is reduced from over 25 to under 12 mg m^{-3} in winter.

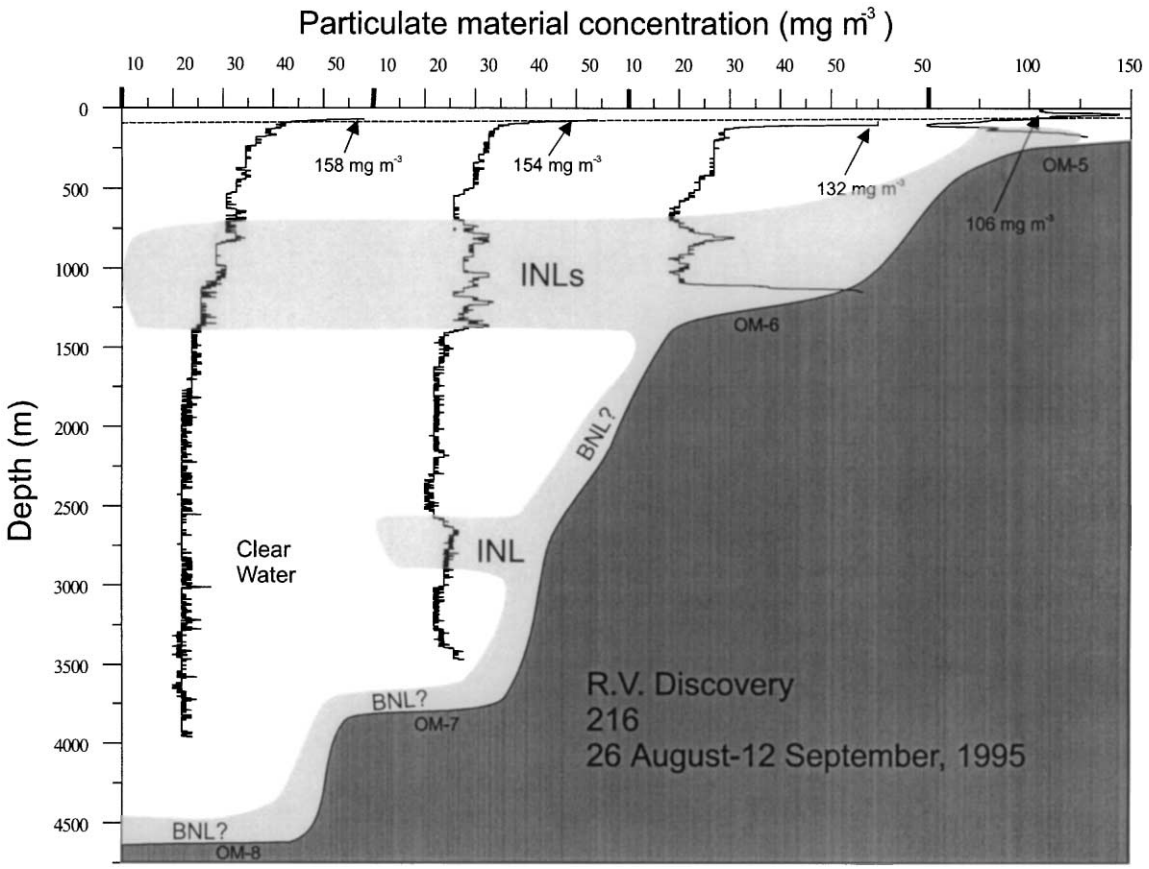

Fig. 6. Turbidity distribution (based on transmission) with depth over Goban Spur sediment trap transect during *D216* (Autumn). Data shallower than 100 m are not shown so as to allow a scale which reveals the structure of the deep water.

3.1.3. *Autumn conditions*

Profiles obtained during *D216* show a return to strong offshore INLs together with the usual structure of surface and bottom layers (Fig. 6). Near-surface concentrations were lower than those found in summer but still elevated compared to winter conditions and showed a slight increase off-slope rising from $\sim 100\,\mathrm{mg\,m^{-3}}$ at station OM-5 to $\sim 150\,\mathrm{mg\,m^{-3}}$ in the deeper OM-7 and OM-8, suggesting primary production.

A single INL was present at station OM-6 between ~ 700 m ($\sigma_t = 27.29$) and ~ 970 m ($\sigma_t = 27.48$) with a peak concentration of $31\,\mathrm{mg\,m^{-3}}$. The INL and BNL structures seen at OM-6 appear to have been laterally mixed off-slope along isopycnal surfaces, as a well formed set of INLs were present at station OM-7 between 660 m ($\sigma_t = 27.30$) and 1450 m ($\sigma_t = 27.74$). The clear water $C_{\mathrm{min(c)}}$ minimum of $\sim 20\,\mathrm{mg\,m^{-3}}$ at both deep stations was lower than seen during the June cruise but certainly higher than in winter. A further INL was present between ~ 2500 and 2670 m with a peak concentration of $27\,\mathrm{mg\,m^{-3}}$ occurring at 2670 m. This deep INL appears to be quite persistent, as a later September cruise (R.R.S. *Discovery* cruise *D217*) also reported its presence.

3.2. Intermittency and offshore transport of INLs

The three surveys described above all show the presence of INLs, albeit of varying structure and intensity, suggesting that they are a common but not permanent feature in the region. Data obtained on R.V. *Poseidon* cruise *P200/7* in summer 1993 (July/August) also confirmed the existence of INLs, while numerous profiles from the region made during R.V. *Pelagia* cruises with similar optical equipment showed no trace of them. The intermittency may arise from periodic generation by stronger currents associated with internal waves and tides that Dickson and McCave (1986) showed to be related to local variations in stratification caused by wind stress and its interaction with topography. This is coupled with rapid advection to the north in the slope current, and spreading offshore in MOW and LDW combined with particle fall-out.

The Atlantic Circulation and Climate Experiment (ACCE) programme has launched many neutrally buoyant floats in the region at the depth of the core of MOW, namely $\sigma_\theta = 27.5\,\mathrm{kg\,m^{-3}}$ or about 900–1000 m depth over Goban Spur. Dr Amy Bower has provided preliminary data that show that most of the floats deployed in the Goban Spur region have tended to move basinward. The 0–60 d trajectories of floats #351 (deployment site depth 1800 m), #331 (2000 m), #326 (4000 m) and #319 (4500 m) were, respectively, to 211° ($2.1\,\mathrm{cm\,s^{-1}}$), 030° ($2.6\,\mathrm{cm\,s^{-1}}$), 210° ($051\,\mathrm{cm\,s^{-1}}$) and 233° ($4.8\,\mathrm{cm\,s^{-1}}$). Only float #331 went along isobaths into Porcupine Seabight, but by 190 d it had travelled west into the basin. The tracks of these floats frequently display looping motion, showing them to have been entrained in MOW eddies or "meddies". The combination of intermittent resuspension under internal waves and slope currents, plus strong meddy-driven basinward transport accounts for most features of the INL field recorded here at depths of 700–1400 m.

This process clearly provides a mechanism for along and off-slope transport of fine sediment material within the OMEX region. However, the relatively low particulate concentration of only $20–30\,\mathrm{mg\,m^{-3}}$ above background in the INLs reported here and absence of INLs reported in other OMEX cruises, suggest that we are missing something contributing to off- and down-slope flux. We will return to this when we have considered results of estimates of large particle abundance.

3.3. Distribution of large particles (aggregates)

3.3.1. Vertical profiles

Previous work has suggested strong diurnal variability in large-particle abundance in the water column (Lampitt et al., 1993a). A test for 24 h at a 1400 m deep station shows no clear diurnal variability and validates the comparisons and cross-sections based here on data taken with the profiling snow camera at different times of day (Fig. 7). Other clear features of this set of profiles are strong subsurface maxima coinciding with (a) the seasonal thermocline and (b) the lowermost 200 m of the BNL. In addition there are other subsurface maxima evident in the particle volume plot. These features are sporadic and have no clear lateral continuity on an offshore profile but are not infrequent features and are also present in regions remote from continental slopes (Lampitt et al., 1993b).

Spatial differences across the slope and temporal differences between seasons in our data are slight. During a long-term deployment at 270 m depth over the Porcupine Abyssal Plain (Lampitt

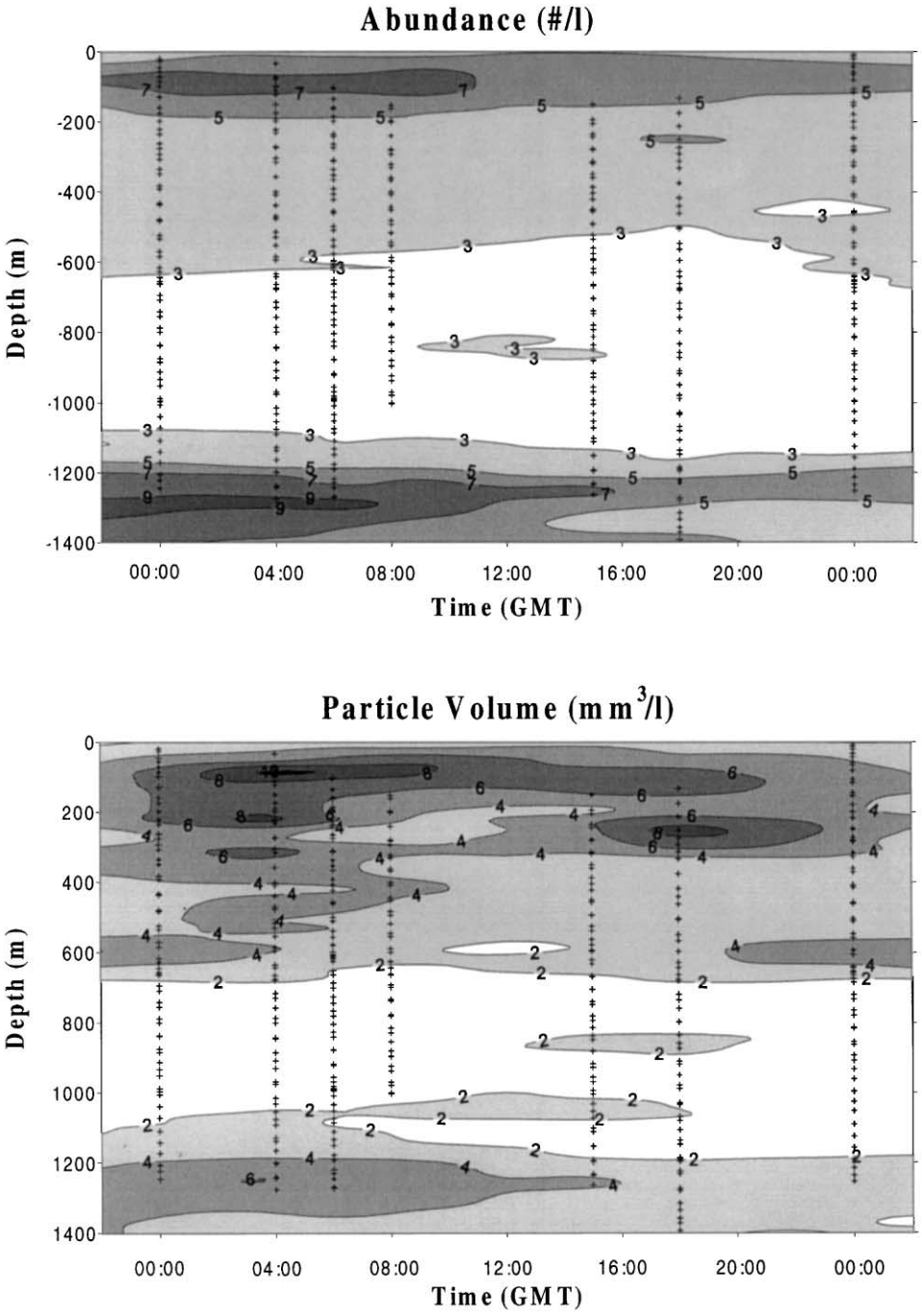

Fig. 7. Contour plot of abundance of particle >0.6 mm in diameter (upper) (number per litre) and volume concentration (lower) (ppm) during a 24 h period at 1400 m depth (49°12′N 12°44′W) in June 1993. Up to 400 data points were obtained in each of the profiles and the location of every 5th one of these is indicated on the plot.

et al., 1993b), there was a factor of 10 increase in total particulate volume during the spring. Without the benefit of such long-term observations, one must assume that by chance none of the cruises coincided with such a peak. The absence of a cross-slope trend (Fig. 8) is more surprising, bearing in mind the higher productivity associated with the shelf break and the higher biomass with decreasing water depth. Reducing the data to an integrated particulate load over the top 1000 m of the water column reveals no significant cross-slope trend but there are significant differences between April and October when values are about $5 \pm 2\,g\,m^{-2}$ and June when they are about $20\,g\,m^{-2}$. This compares with estimates via transmissometer of about $17\,g\,m^{-2}$ in October and $34 \pm 3\,g\,m^{-2}$ in June. The increase due to the spring bloom has a greater impact on the large particle population than the fine, as might be expected.

3.3.2. *Variability in the benthic boundary layer*

Fig. 9 shows mean values *plus* standard deviations of particle concentrations in the BBL (0.05–0.40 m.a.b.) under different flow conditions. They reflect a spring/summer and an autumn/winter situation and revealed the following trends (a) during autumn/winter cruises (October and January) spot measurements at 0.30 m.a.b. of averaged flow speeds varied between 8 and $37\,cm\,s^{-1}$ (Fig. 9A, black dots), (b) flow speed increased from the shelf station to OMEX-II (1470 m), where the highest values of 35–$37\,cm\,s^{-1}$ were determined during the two cruises, and (c) between 1470 and 3600 m the flow speed decreased to $8\,cm\,s^{-1}$. Replicate measurements

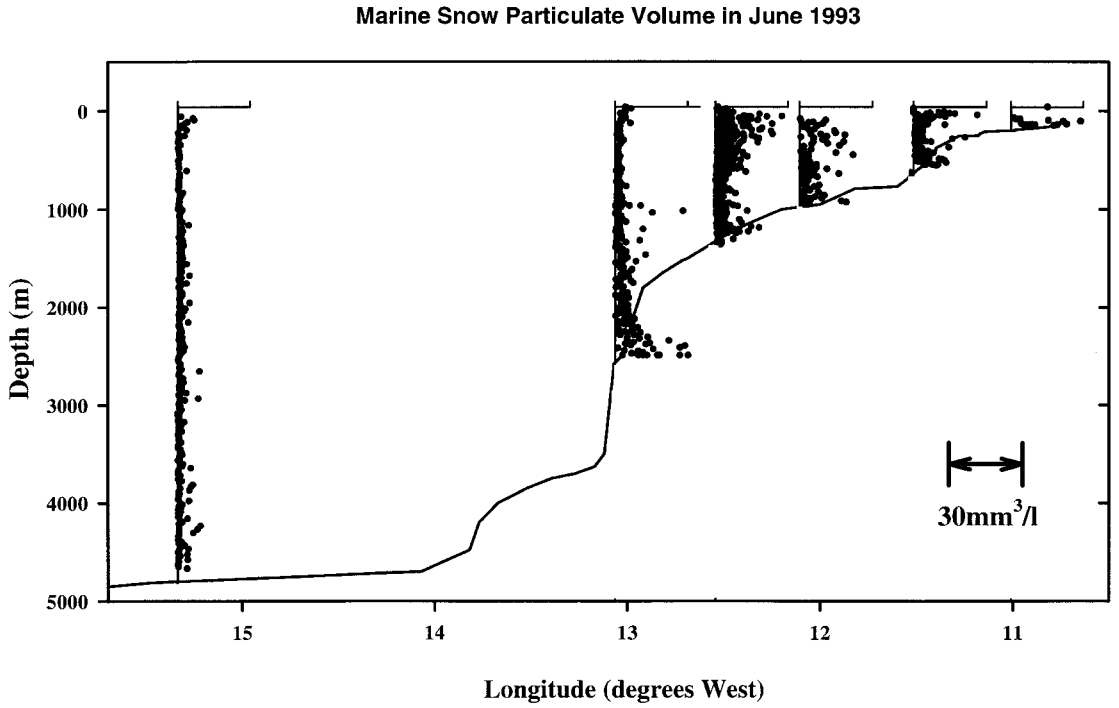

Fig. 8. Vertical profiles of marine snow volume concentrations across Goban Spur in June 1993 obtained from the large particle camera. Minimum recorded size 0.6 mm.

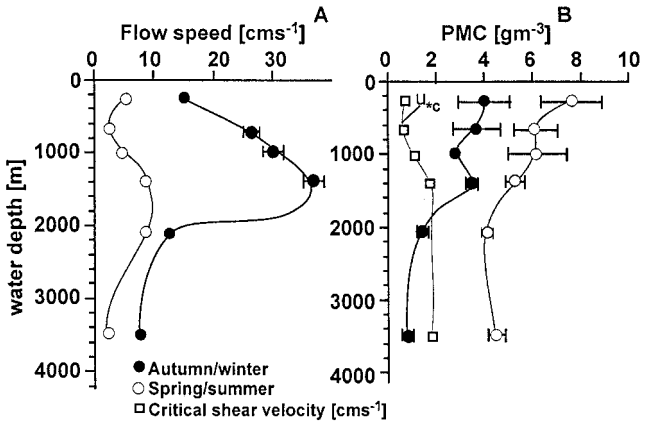

Fig. 9. Spatial and temporal variability of particulate matter in the benthic boundary layer (0.05–0.40 m.a.b.) at Goban Spur. Data are means from spring/summer, autumn/winter cruises sampled along the OMEX transect during at least two cruises and including standard stations sampled during all cruises. Black dots represent winter/autumn cruises, circles represent spring/summer cruises. A: Flow speed at 0.30 m.a.b.; B: Suspended particulate material at different heights and shear velocity based on 2-point velocity profiles.

during the various cruises at the shelf station and at OMEX-II gave similar values. During spring/summer cruises (May and August/September) flow speeds did not exceed $10\,\mathrm{cm\,s^{-1}}$ (Fig. 9A, open dots). Again the highest flows (up to $8.5\pm0.9\,\mathrm{cm\,s^{-1}}$) were found at the upper slope with decreasing values at the lower slope and lowest values of $1.5\pm0.1\,\mathrm{cm\,s^{-1}}$ at 4500 m-water depth. Light attenuation coefficient ranged from 0.650 to 0.840 (equivalent to 278–464 $\mathrm{mg\,m^{-3}}$ on our calibration). Particulate matter concentrations decreased with depth during summer and autumn (Fig. 9B). Despite higher flow velocities in autumn, PM in the BBL was $\sim$50% lower than in summer. The highest PM concentrations occurred at stations with the lowest critical shear velocity (Fig. 9B). The data of Thomsen and van Weering (1998) show that critical erosion shear velocity ($u*_{cr}$) increased with depth from 0.48 to $1.65\,\mathrm{cm\,s^{-1}}$. Between 1000 and 1470 m, $u*_{cr}$ doubled from 0.8 to $1.6\,\mathrm{cm\,s^{-1}}$.

3.3.3. *Particle size and settling velocity in the benthic boundary layer*

On the shelf the median aggregate size (measured by particle cameras) varied between 0.34 mm (resuspended sediments) and 0.47 mm (5.0 m.a.b.), and the highest number concentrations of up to 1.152×10^{6} large particles $>100\,\mu\mathrm{m\,m^{-3}}$ were observed there. Under low flow conditions at OMEX-I (670 m water depth), the largest aggregates were found with median diameters of 0.31–0.47 mm and maximum sizes of up to 1.40 mm. The aggregate size in the BBL between 0.2 and 0.4 m.a.b. *increased* away from the bed, with number concentrations of $0.470–0.380\times10^{6}\,\mathrm{m^{-3}}$ (Table 1).

A narrow aggregate size spectrum without significant differences in aggregate diameter was observed at 1470 m water depth, where the highest flow velocity was measured (Fig. 9A). The median aggregate size varied between 0.20 and 0.27 mm, and no aggregates larger than 0.70 mm were found. Aggregate number varied between 0.109 and $0.270\times10^{6}\,\mathrm{m^{-3}}$. The median

Table 1
Median aggregate size d_{50} (mm) and numbers per litre (n l^{-1}) in the BBL in August 1995[a]

Station	Depth (m)	$u*$ (cm s^{-1})	Resuspended A (mm)	Resuspended B (mm)	0.2 m.a.b. (mm)	0.2 m.a.b. (n l^{-1})	0.4 m.a.b. (mm)	0.4 m.a.b. (n l^{-1})	5.0 m.a.b. (mm)	5.0 m.a.b. (n l^{-1})
OMEX-A	380	0.36	0.34	0.100	0.37	1152	0.38	770	0.47	1020
OMEX-I	670	0.13	0.31	0.090	0.38	470	0.47	380	0.44	446
OMEX-B	1000	0.31	0.36	0.054	0.41	282	0.30	278	0.44	188
OMEX-II	1470	0.57	0.22	0.018	0.27	270	0.20	190	0.21	109
OMEX-F	2000	0.53	0.30	0.012	0.36	323	0.28	244	0.30	224
OMEX-III	3600	0.15	0.19	0.010	0.15	248	0.18	250	0.33	244
OMEX-E	4500	0.11	0.30	0.008	—	—	0.18	338	0.27	101

[a] Shear velocity $u*$ is based on a two-point velocity profile. "Resuspended" sediments are the median particle sizes of surface sediment which were resuspended during touch down of BIOPROBE. Resuspended sizes, A: measured with the particle camera and B: measured with a Coulter Counter (disaggregated).

(disaggregated) sediment grain size (measured by Coulter Counter) was 18 μm. The same trend, but with higher median sizes and abundances, was observed under similar flow conditions at station OMEX-F (2000 m).

At OMEX-III (3600 m), despite similar flow conditions to 670 m depth, large aggregates (0.33 mm, 0.144×10^6 m^{-3}) were only found at 5.0 m.a.b. and the resuspended sediment surface particles were larger (0.19 mm) than aggregates at 0.2 m (0.15 mm) and 0.4 m (0.18 mm). The median (disaggregated) sediment size was 8 μm. Under the lowest flow conditions at OMEX-E (4500 m water depth), the sediment bed was covered with particles of diameter about 0.30 mm (disaggregated size $d_{50} = 10$ μm), whereas aggregates transported in the BBL were 0.18–0.27 mm in size.

Chloroplastic pigments were found at the deepest stations. The rapidity of transport is indicated by a half-life of 23 d for Chlorophyll a in fresh phytodetritus (Graf et al., 1995). Phytodetritus aggregates had settling velocities of 0.5–1.6 cm s^{-1} (430–1380 m d^{-1}), greater than values normally associated with water-column aggregates (Alldredge and Gotschalk, 1988) (Fig. 10). The cause is high lithogenic content in the resuspended aggregates originating in high lithogenic content of the bed. It confers the possibility of rapid downslope transport on the steep outer slope of Goban Spur, particularly when associated with strong downslope flow components outlined below (Pingree and Le Cann, 1989; Thomsen and van Weering, 1998).

The observed concentration ranges in the BBL, which are much greater than those in the overlying water column, are in the same order of magnitude as reported from the BBL on other European continental margins, such as the western Barents Sea and the North East Greenland Sea (Thomsen and Graf, 1995; Thomsen and Ritzrau, 1996; Ritzrau and Thomsen, 1997). The PM concentration was of the same order of magnitude as reported for the deep sea during benthic storms under similar flow conditions (Gross and Williams, 1991). The high BNL concentrations at 0.1–0.4 m.a.b. (up to 10 × higher than those at 10 m.a.b. determined optically) are consistent with expected aggregate distribution in the boundary layer. For example, in a BBL with shear velocity $u* = 0.5$ cm s^{-1} and aggregates of settling velocity $w_s = 0.1$–0.2 cm s^{-1}, the Rouse Number $\beta = w_s/\kappa\, u*$ (where κ is von Karman's constant, 0.4) is 0.5–1, indicating a steep gradient. With this β

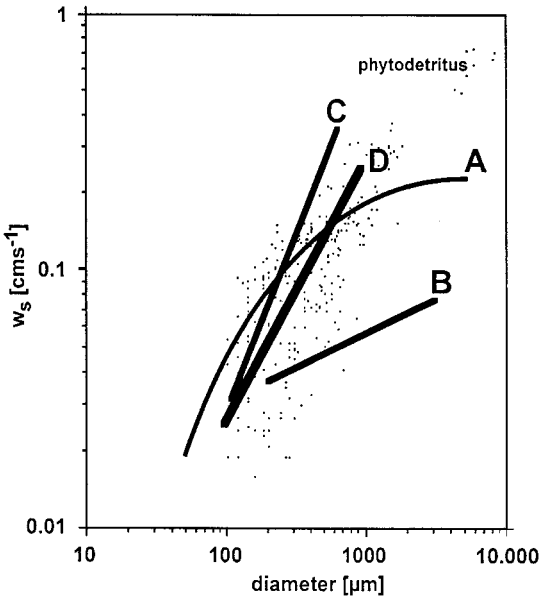

Fig. 10. Ranges of sizes (μm) and settling (cm s^{-1}) velocities of aggregates in the benthic boundary layer at Goban Spur compared to the empirical relationships of: A, McCave (1984); B, Alldredge and Gotschalk (1988); C, Sternberg et al. (1999); and D, (data-points: BBL aggregates and phytodetritus, fluff), Thomsen and van Weering (1998).

the concentration of aggregates at 1.0 m.a.b. is 0.1–0.32 of that at 0.1 m.a.b., and at 10 m.a.b. it is 0.01–0.1. The aggregates are confined to the lower part of the optically detected nepheloid layer. Although the BIOPROBE data are only spot measurements with no coverage of tidal cycles, the short-term data are consistent with short-term data from the STABLE tripod (Chatwin, 1996) and long-term BBL data from the NIOZ BBL lander "BOBO" (Thomsen and van Weering, 1998).

3.4. Downslope flows in the boundary layer

STABLE made high-frequency measurements (with electromagnetic current meters) of near-bed current profiles during 21–31 January 1994 at a depth of 879 m where the combination of stratification and bottom slope was near optimal so that intensified internal waves at a wide range of frequencies might be expected. Bottom stresses have been estimated by Chatwin (1996) from the profiles, yielding maximum shear velocities of $u* \sim 1.3\,\mathrm{cm\,s^{-1}}$ but more typically $0.5\,\mathrm{cm\,s^{-1}}$ at the peak of the dominant tidal currents. In comparison, Pingree and Le Cann (1989) fitted a logarithmic profile to instantaneous near-bed currents at 530 m depth on the west flank of a canyon (48°12.9′N, 9°11.7′W, where tidal currents are stronger) to obtain $u* = 1.8\,\mathrm{cm\,s^{-1}}$. Maximum flow velocities exceeding $15\,\mathrm{cm\,s^{-1}}$ measured by the BOBO lander occurred more frequently in 1994 and were directed dominantly down-slope with increasing values, occasionally exceeding $20\,\mathrm{cm\,s^{-1}}$, in late summer and autumn. The averaged drift downslope at site F (2600 m,

northern transect) of $10\,cm\,s^{-1}$ ($u* \sim 0.8\,cm\,s^{-1}$) is too high for the sedimentation of fine aggregated particles with w_s of up to $0.2\,cm\,s^{-1}$ (assuming that particles of $w_s < 0.64u*$ are not deposited (Allen, 1971)). These estimates suggest that significant sediment accumulation on the lower slope is due to downslope transport in, and deposition from, the BBL. Progressive resuspension loops within the benthic boundary layer would result in long-term downslope fluxes of fine particles including POC (Thomsen and van Weering, 1998, Fig. 5)

4. Trapped particle fluxes

Moorings with two and three Kiel-type traps, respectively, were set at sites OMEX-II and -III between July 1993 and September 1994 (Antia et al., 1999, 2001). Traps were at 600 and 1050 m (II) and 580, 1440 and 3220 m (III) where water depths are 1445 and 3650 m, respectively, (Fig. 11). The lower traps were thus at least 400 m above the bed and out of the BNL. Current speeds were mainly below $20\,cm\,s^{-1}$ and trap inclinations were $<4°$; thus current effects are considered slight (Gardner, 1985; Baker et al., 1988: Gardner et al., 1997). Nevertheless there is unavoidable error in the trapping procedure and the uncertainty of calculated fluxes is difficult to partition between trapping and analytical sources. Annual ^{230}Th and ^{210}Pb measurements at OMEX-III indicate that sampling efficiency was in the range 80–120% for the 1440 and 3220 m traps (Antia et al., 1999). Undersampling may have been more severe for the 580 m trap, though its extent cannot be determined due to trap clogging in spring and thus incomplete temporal coverage (Antia et al., 1999).

The trapped fluxes of four components are shown in Fig. 11. Despite the probable errors in absolute values they are internally consistent, allowing us to obtain ''lateral fluxes''. The ''lateral flux'' is defined as the difference between the measured flux at a trap and the flux that would have entered that trap by settling from the next trap above (taking into account dissolution or remineralisation that would have occurred en route). The latter calculations are made for POC and carbonate fluxes. There are several clear trends: (a) trapped fluxes tend to increase with depth and (b) there is a significant inferred lateral input flux of mineral components at the OMEX-III 1440 m level of 75–95% of the flux, and similarly but somewhat less at OMEX-II 1050 m, while at the deeper OMEX-III trap it is only 20–30% of the total.

4.1. Lithogenic material and opal

Lithogenic and opal fluxes are straightforward. The fluxes of lithogenic material are dominated by lateral transport off the continental slope, which contributes up to 93% at 1400 m (OM-III) (Fig. 11A). This is only to be expected as there is negligible sea surface source for this material, the wind blown flux being less than $0.6\,g\,m^{-2}\,a^{-1}$, the value measured by the 600 m trap at OM-III. (Most of this may actually be laterally supplied from shelf-edge resuspension at ~ 180 m depth.) Considering the vastly different time scales of 1 year for water column flux and later Holocene (7000 years) average for deposition, there is a surprising consistency between the measurements. A significant amount of the opal is also transported laterally (up to 74% at OM-II, 1400 m), but this material is almost entirely dissolved on the seabed and contributes only rare diatoms to the sedimentary record (van Weering et al., 1998) (Fig. 11B).

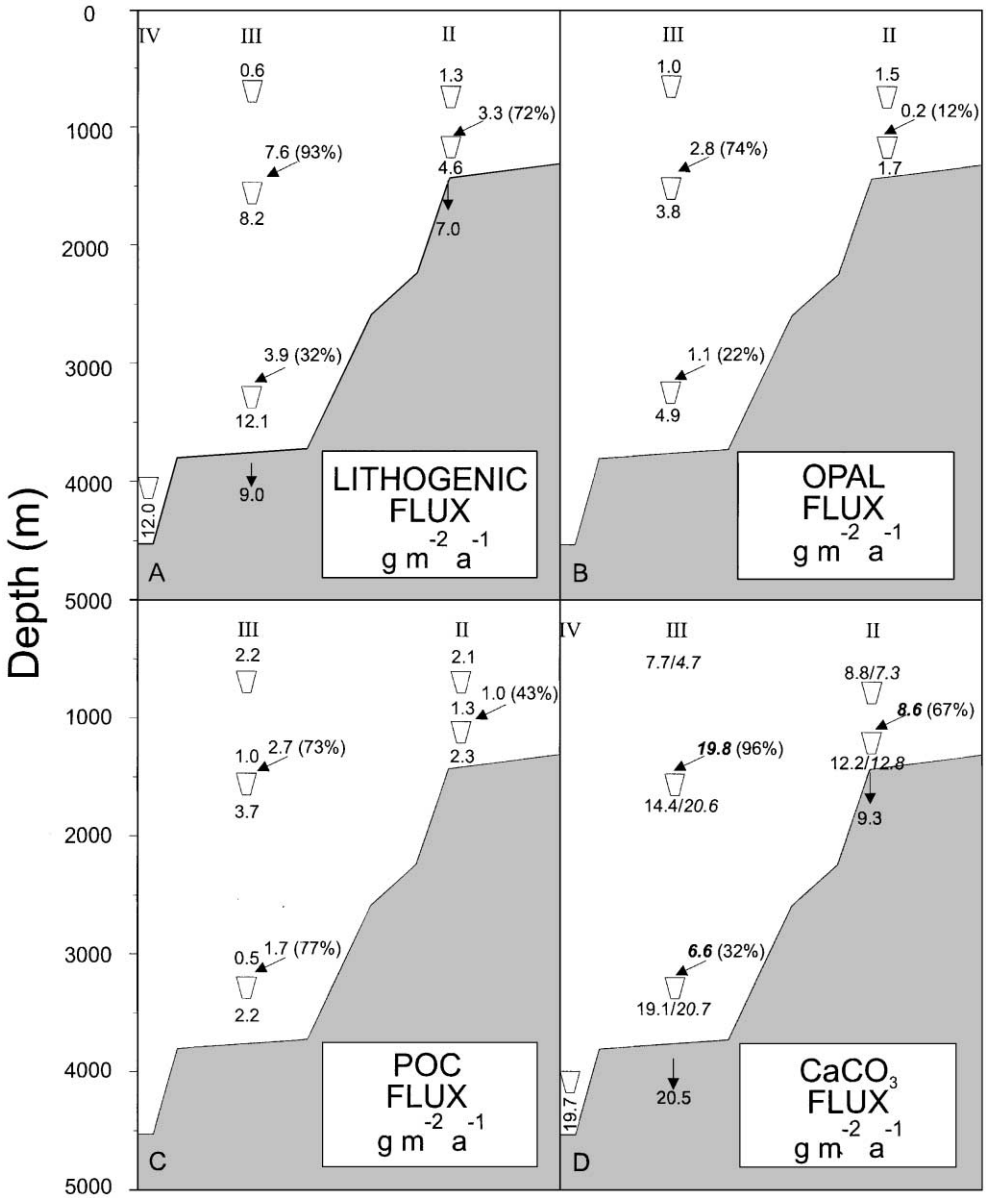

Fig. 11. Annual trapped vertical and inferred lateral fluxes (by arrows) at the Goban Spur sites OMEX II (1440 m) and OMEX III (3450 m). A. Lithogenic flux. Obtained by Wollast and Chou (1998) as 14.3 [Al]. Indicated "lateral" fluxes are the difference between trap accumulation and input from the trap above. B. Opal flux (calculated from [Si] assuming 10% water content) by Antia et al. (1999). Lateral fluxes as in A. C. POC flux. Input fluxes to lower traps are calculated assuming the upper ($\sim$600 m) trap collects only vertical flux with a vertical degradation rate given by the relationship of Martin et al. (1987). "Lateral" fluxes are the difference between the calculated input flux (allowing for degradation) and the measured trap accumulation. D. Calcium carbonate flux. Obtained by Antia et al. (1999) as 8.33 PIC and Wollast and Chou (1998) as 2.5 [Ca] (bold).) Lateral fluxes take account of $CaCO_3$ dissolution via the ratio with lithogenics; see text and Wollast and Chou (1998).

4.2. Carbon and carbonate fluxes

Particulate organic carbon fluxes (Fig. 11C) also show significant lateral enhancement at both mid-water and deeper levels. This calculation is based on the measured flux into the top trap (assuming none is lateral) taken to represent the export flux from the mixed layer, and the VERTEX equation of Martin et al. (1987), which describes vertical trends in flux. At OMEX-III this is possibly an overestimate due to incomplete spring sampling at 580 m. Although the equation of Martin et al. (1987) is based on open-ocean data, the depth dependence represented by the exponent $b = 0.858$ is almost identical to the depth dependence at a nearshore site ($b = 0.863$) in an earlier experiment in the same region (PREVTX) given by these authors. If vertical input is calculated from estimates of new production (export flux through 100 m), the calculated lateral input is somewhat lower. The composition of POC in the intermediate traps and its relative "freshness" indicated by chloroplastic pigment and organic biomarker concentrations show that this lateral transport must be rapid, compared to particle degradation rates (Antia et al., 2001).

There are notable differences (up to 40–60%) in the estimates of carbonate flux due to method (compare values in Fig. 12D). The reasons for these differences are not clear. Values from Wollast and Chou (1998) are calculated from measured particulate [Ca] whereas those from Antia et al. (1999) result from conversion of particulate inorganic carbon (PIC) to $CaCO_3$. Carbonate fluxes estimated from PIC might, to a small extent, reflect the inclusion of Mg-

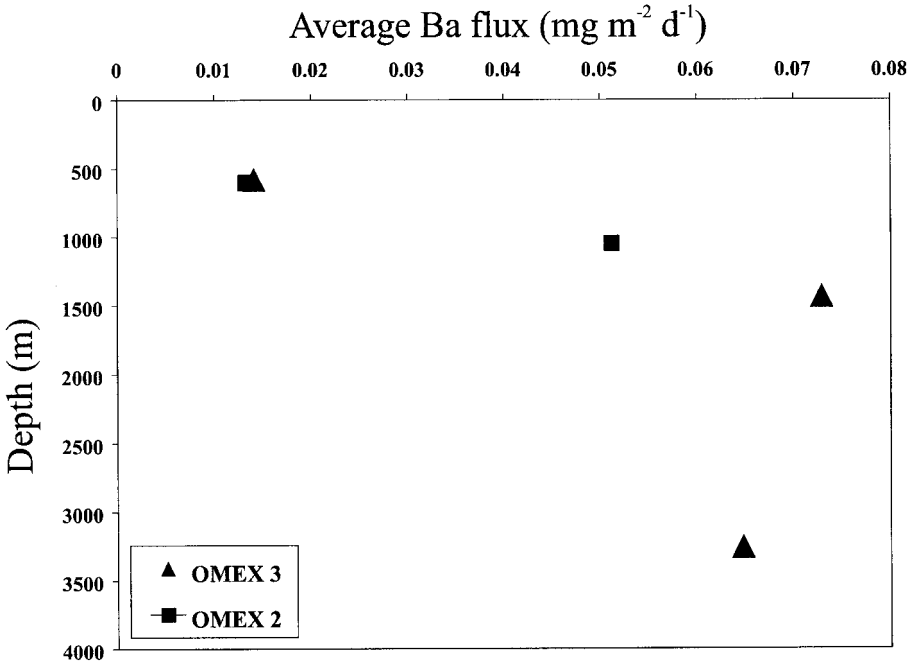

Fig. 12. Year averaged daily Ba fluxes (mg m^{-2} d^{-1}). Squares, OMEX-II; triangles, OMEX-III; (see also Dehairs et al., 2000).

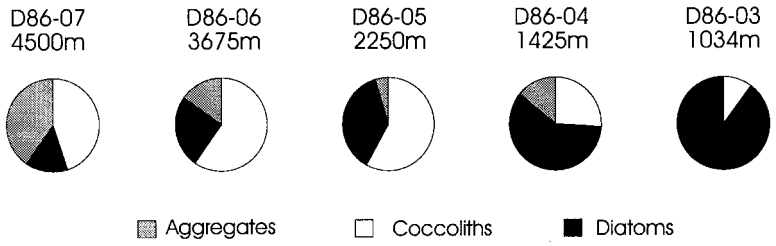

Fig. 13. Variation in the relative abundance of coccoliths, diatoms and aggregates in bottom nepheloid layer suspended particulate matter along the Goban Spur northern transect in May 1994. Relative abundance was determined from the area percentage on filters covered by the different components examined under the SEM. Depth indicates water depth of bottom sampling stations along the Goban Spur. Samples from bottles on CTD $\sim$10 m.a.b. Station positions given on Fig. 1.

and Sr-calcite in the analysis, however, this cannot occur at a magnitude able to explain the differences seen.

The POC fluxes measured were very similar to those found 200 km to the north at a water depth of 2000 m in Porcupine Sea Bight (Lampitt et al., 1993b) with values of 1.8 and 1.6 g m^{-2} a^{-1}. Near bottom elevation in the POC flux of similar magnitudes also were found. The calcite flux in the Porcupine Sea Bight was also similar at 14 g m^{-2} a^{-1}, and both values are within the range of those found at these latitudes in the open ocean of 7–18 g m^{-2} a^{-1}. Both Honjo and Manganini (1993) and Newton et al. (1994), show, in trap data from 2000 to 3750 m depth at the latitude of Goban Spur, very similar values for fluxes of $CaCO_3$ (12–15 g m^{-2} a^{-1}), opal ($\sim$5) and POC (1–3), to those recorded here. Lithogenic fluxes are small and increase downwards from an estimated 0.4 g m^2 a^{-1} at the surface to 1.3 g m^{-2} a^{-1} at 3750 m in Honjo's data at 48°N, 21°W (Honjo, 1996) (Honjo records the flux as 1.3 g m^{-2} a^{-1} by weight but 159 mgAl m^{-2} a^{-1}. The factor Al $\times$ 14.3 = lithogenic from Martin and Whitfield (1983) used here and by Wollast and Chou (1998) would give 2.3 g m^{-2} a^{-1}). The Goban Spur is not very different in its characteristics from other nearby slope environments in terms of the primary vertical flux and the delivery of carbon, carbonate and opal to the seabed. Furthermore the slope environment seems to affect primary vertical flux rather little and is only distinctive in having significant lithogenic flux, mainly laterally supplied.

Temporal variation in the fluxes is shown by Antia et al. (1999) and Wollast and Chou (1998) to have the expected features of a spring bloom period of high flux in late April to early June and a late summer/early autumn higher flux period also. These are seen in organic matter, carbonate and lithogenic material at all trap depths. There is also a mid-December to mid-January increase in lithogenic flux, also at all depths but particularly the deeper ones. Since the fluxes here are dominated by lateral supply, coincidence with blooms implies that these events were related to some changes at the bed, possibly the biological effects leading to increased resuspension observed by Thomsen and Flach (1997). The winter pulse of lithogenic flux was most likely due to storm activity on the outer shelf for the shallower traps, and perhaps deep penetration of storm energy (Dickson et al., 1982, 1985) causing resuspension on the slope to supply the increased flux seen at the deeper ones.

4.3. Dissolution of $CaCo_3$

The calcium carbonate flux is investigated in further detail by Wollast and Chou (1998). Assuming the lithogenic material (estimated via [Al]) to be conservative, i.e. not subject to precipitation or dissolution, there appears to be a significant degree of dissolution of $CaCO_3$ in the water column below 200 m. The composition of in situ filtered samples shows fairly constant lithogenic concentration with depth but a rapid decrease in $CaCO_3$ content in the upper 200 m (due partly to aggregation and removal of coccoliths) and continuing gradual decrease of the proportion of $CaCO_3$ concentration relative to lithogenic down to 1200 m (due significantly to dissolution). Thus carbonate is clearly not conservative in the water column, a fact pointed out by Bishop et al. (1980) and revived by Milliman (1993). Apart from its implications for continental margin carbon budgets, this fact also may indicate discrepancies between the relative abundance of different coccolith species in surface waters and their preserved record, even when well above the lysocline.

Assuming conservative behaviour for fluxes of lithogenic material, and depth-dependence for $CaCO_3$, any depth may be characterised by a $CaCO_3$/lithogenic concentration ratio. If this ratio is given by its value for trapped material at that depth, then just as the lithogenic material in a trap can be divided into that settling from the level of the trap above and lateral input flux, so the associated lateral carbonate fluxes can be assessed from the lithogenic flux and the lithogenic/$CaCO_3$ concentration ratio. By this means, Wollast and Chou (1998) calculate the lateral supply of carbonate to be greater than that given by the flux difference between two traps one above the other because there is dissolution en route. The estimates of lateral $CaCO_3$ flux on this basis are given on Fig. 11D. The net effect of this dissolution may be gauged from the estimated $CaCO_3$ production of $100\,gCaCO_3\,m^{-2}\,a^{-1}$ (based on primary productivity of $160\,gC\,m^{-2}\,a^{-1}$, Joint et al., 2001) and the deep trap records of $13–21\,gCaCO_3\,m^{-2}\,a^{-1}$). Seabed burial fluxes of $9–21\,gCaCO_3\,m^{-2}\,a^{-1}$ at the trap sites are consistent with this, and both sets of figures suggest that 80–90% of the carbonate originally fixed by organisms is dissolved in the water column.

4.4. Biogenic barite

Barium flux has been examined by Dehairs et al. (2000) and shown, in common with other components, to increase with depth (Fig. 12). The accumulation rate of biogenic Ba (Ba_{bio}) in traps just above the BNL is 6–7 times that at 600 m. There must be significant lateral flux plus the possibility of precipitation of barite within sinking organic matter. It is clear that if Ba increases downwards, for whatever reason, the flux of Ba_{bio} through the water column as well as its accumulation in bottom sediments will not be straightforwardly related to primary productivity of the overlying waters as postulated by Dymond et al. (1992) and Francois et al. (1995). This problem is particularly likely to occur at continental margins. Dehairs et al. (2000) also noted a seasonal shift in the flux-weighted POC/Ba_{bio} ratio in shallow (600 m) traps, from 600 to 800 in summer and autumn to 150–500 for the rest of the year. This probably points towards a seasonal variability in the efficiency of the barite production process. However, since export production calculations are based on yearly averaged Ba fluxes, the impact of such seasonal variability is probably small, although for Ba_{bio} to become a reliable tracer of export production, the underlying reasons for this seasonal variability of the POC/Ba_{bio} ratio need to be understood

(Bishop, 1988). Furthermore, proper evaluation of the lateral advection component of Ba_{bio} is required when using either trap or bottom sediment Ba data to estimate palaeoproductivity, especially on continental margins—particularly coastal upwelling systems.

5. Particle properties under SEM

The SEM observations of filtered PM indicate a change in composition of the particles contained within the BNL along the transect (Fig. 13). At the shelf and upper slope, diatoms and diatom fragments are the dominant particles in the BNL, at slope margin station D86-04 aggregates and faecal pellets together with coccoliths become increasingly important, and deeper down the margin (partially corroded) coccoliths and aggregates are dominant. Filters collected in May/June 1994 were very rich in diatoms, whereas the September 1995 filters contained considerably less material (Fig. 14).

In general, the SEM images of particles collected on Nucleopore filters show both individual and multiple-grain particles with components of both mineral and organic origin (Fig. 14). In addition to clastic terrigenous minerals, individual grains within the silt and clay size range ($<63\,\mu m$) include single coccoliths, and skeletal fragments of diatoms, radiolaria and sponges. Multiple-grain types include all of the aggregate forms (open, close and tight) described by McCave, 1985 from the HEBBLE area on the Nova Scotian Rise and Richardson (1987); Richardson and Hollister (1987) on the Iceland Rise and US Margin SE of New York.

6. Lateral fluxes and sources of aggregates

The evidence from both traps and PM concentration profiles is that there must be substantial transport of material off the slope shown by the inferred lateral fluxes in Fig 11. At the outset we observe that it appears unlikely that this flux totalling $46\,g\,m^{-2}\,a^{-1}$ at OM-III can be obtained from the observed dilute INLs with fine particles, which are only about $20–30\,mg\,m^{-3}$ above background. Aggregation time scales for fine-grained dilute nepheloid layers are weeks to months (McCave, 1984; Thomsen and McCave, 2000). The ratio of depositional residence to scavenging times in the BNL for $10\,\mu m$ particles at 10 m.a.b. is only 6×10^{-3} (Thomsen and McCave, 2000). For $5\,\mu m$ particles that ratio would become about 2.5×10^{-2}, still indicating that BNL particles stand a much higher chance of being lost from suspension by depositional fall-out than by scavenging through contact with large aggregates. An INL is like a BNL but without boundary turbulence and with a base that allows complete and unimpeded removal of particles, i.e. they all sink through it. The INLs are thin relative to the total water column, a few hundred metres at most, so only a very large flux of primary aggregates from the sea surface would have much scavenging effect: an aggregate does not spend sufficient time in an INL to scavenge much. Significant scavenging by sinking large particles would imply a much larger flux of them from the surface than is measured by the 600 m traps.

The only viable solution to the lateral flux problem is that the INLs also contain, for a brief period after their generation by detachment of a BNL, a population of large, fast-sinking particles. Such a population is detected in the BNL (Table 1, Fig. 8) (Thomsen and van Weering,

1998), and there are also mid-water patches of higher volume concentration of large particles (Fig. 8). What we detect in INLs is simply the fine smoke after the shot has been fired! The INL signal is mainly due to fine particles—Dickson and McCave (1986) show a very large signal measured by light scattering, but generally the signal is much smaller when measured by transmission. The notion that INLs are created by the detachment of BNLs implies that they start off with BNL properties, and, as demonstrated by Thomsen and van Weering (1998), this includes high near-bed concentration and large particles with settling velocities in the region of 0.03–0.15 cm s^{-1} (and some resuspended phytodetritus aggregates of 0.25–1.5 cm s^{-1}). It is about 45 km from the top of the slope at which resuspension could occur, to the 1450 m trap at OMEX-III. Travelling at 0.1 m s^{-1} offshore, a particle of $w_s = 0.1$ cm s^{-1} would sink 450 m from the point of resuspension. A particle of 0.03 cm s^{-1} sinking speed would settle 135 m. That would put points of origin between 1000 and 1315 m depth, a region of pronounced BNLs and INLs (Figs. 4 and 5). However it seems unlikely that the fast-sinking phytodetritus aggregates would get out to the trap depth unless they were broken up during an intense resuspension event. This process of resuspension and offshore transport must be intermittent, and probably related to activity of both internal waves and large-scale deep eddies. Antia et al. (1999) measured spikes in light attenuation at the traps which indicate that they were periodically enveloped in INLs.

Fig. 14. SEM images of suspended sediment on Nucleopore filters collected in clear water and nepheloid layers in winter, summer and autumn. (a), (b) Winter (January, 1994). (a) Depth 2751 m, station OM-8, associated with $C_{min(c)}$ (11 mg m^{-3}). The image shows a general scarcity of particles, with those present mainly individual clay particles and a few pieces of diatom. (b) Depth 1134 m, station OM-8. Transmissometry, nephelometry and gravimetric analysis indicate an INL (41 mg m^{-3}) at this depth. Contrast with the $C_{min(c)}$ picture of Fig. 14a in showing abundant individual grains of coccoliths, diatom fragments, clay and silt particles, tight aggregates and some organic debris. Higher magnification images of particles from the BNL of station OM-8 show the presence of diatoms. (c), (d), (e) Summer (June, 1995). (c) Depth 500 m, station OM-7. This is below the SNL but within the depth range of generally enhanced SPM concentrations. In this case the filter is blocked with large organic patches of mucus some several hundred micrometres in diameter, which on closer examination show embedded particles of coccoliths, silt and clay. The disaggregation of such particles as they fall towards the seabed may be important in generating the seasonal shift in clear water concentrations. (d) Depth 1847 m, station OM-7. Clear water. The difference between this and the winter material in clear water (a) is quite marked. There are abundant individual particles comprising coccoliths, silt and clays together with skeletal fragments of diatoms, radiolaria and sponges. There are also both closed and open form aggregates with some evidence of mucus. The presence of sponge spicules in the samples is of particular interest because the biomass of sponges is notably high between 500 and 1000 m on the slope in the region of enhanced resuspension. The clear water material also reveals a number of faecal pellets (tight aggregates), typically $\sim$70 μm in diameter and having lost their peritrophic membrane. Similar characteristics are seen in an off-slope sample taken at 2751 m at station OM-8. (e) Depth 1489 m, station OM-10. This sample is from the peak concentration in the rather weak BNL of $\sim$30 mg m^{-3}. It shows a greater proportion of individual particles and fewer aggregates than in clear and upper water column samples. The single grains are compositionally similar to the samples from points higher up in the water column. Aggregates are present (upper right) but are somewhat smaller than previous. Skeletal fragments of sponges are also present, and a dark blob of mucus is present lower centre where the holes of the filter are covered over. (f), (g), (h) Autumn (September, 1995). (f) Depth 900 m, station OM-6, from just below the peak concentration in the INL at this depth. The majority of material is associated with open aggregates comprising coccoliths and silt particles. There are also a number of intact dinoflagellates. (g) Depth 1186 m, station OM-6, BNL. Abundant individual grains of silt and clay size. Aggregates of all forms are present. (h) Depth 1186 m, station OM-6, BNL. Tight structures are thought to be either faecal pellets or resuspended lumps of the bed. There exists a significant amount of organic debris and some mucus present in these aggregates which could mean they are faecal pellets.

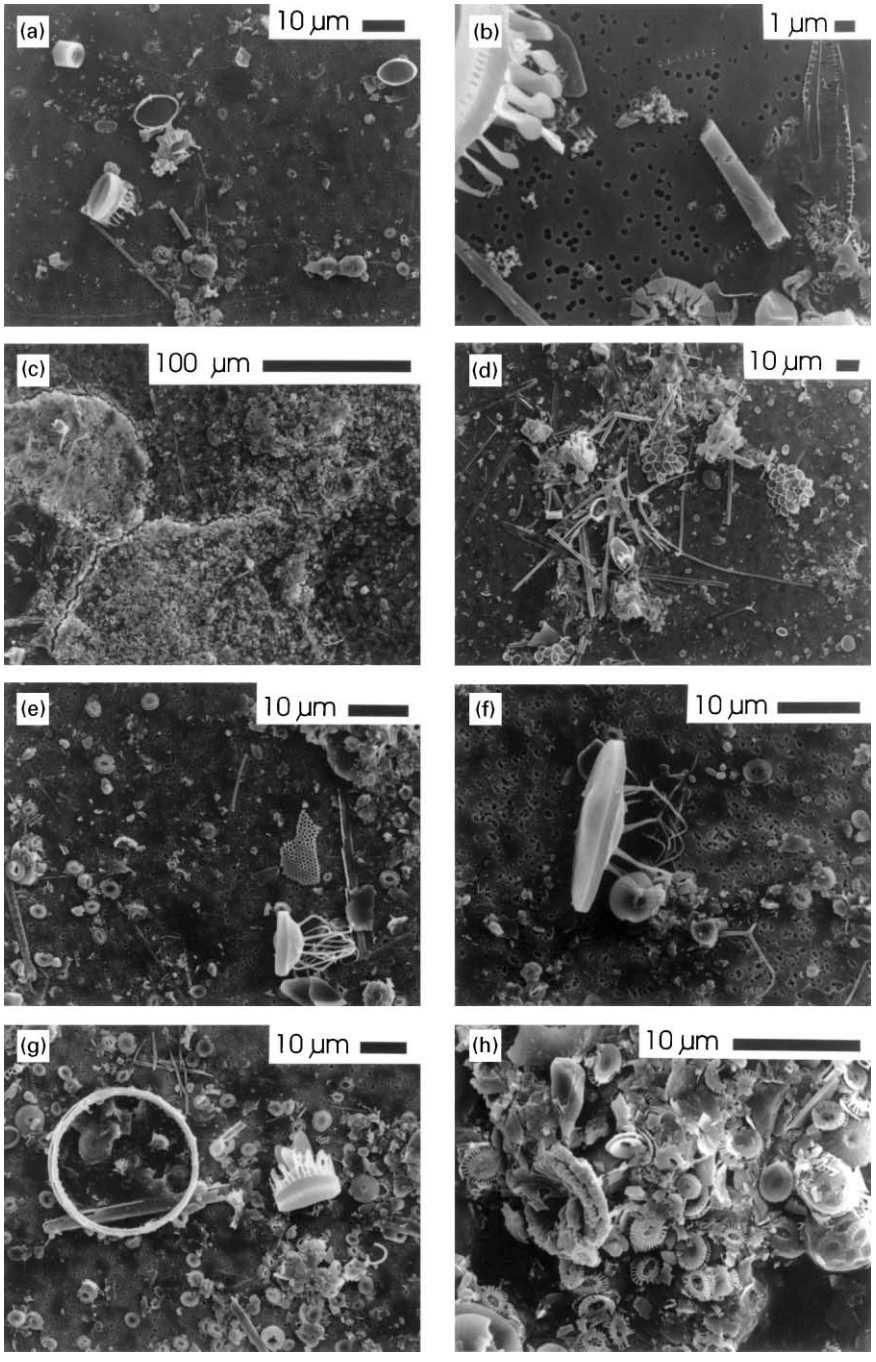
(a)
10 µm
(b)
1 µm
(c)
100 µm
(d)
10 µm
(e)
10 µm
(f)
10 µm
(g)
10 µm
(h)
10 µm

However the large particle fall-out to the traps is more likely to have occurred from INLs situated a few hundred metres shallower. The deeper mid-water trap at OMEX-3 (1440 m) is thus better situated to catch more of the INL fall-out than is the shallower counterpart at OMEX-2 (1050 m), which catches a lower flux due to being periodically above the main INL level.

7. Summer to winter clear water changes

In the Atlantic, the clear water particle concentration is commonly between 5–20 $mg\,m^{-3}$ (Brewer et al., 1976). The spatial variation shown by the Lamont group (Eittreim and Ewing, 1974; Eittreim et al., 1976; Biscaye and Eittreim, 1977) appears to depend mainly upon the productivity of the surface waters. Here at the deeper stations we see a temporal difference between summer and winter of about 10–15 $mg\,m^{-3}$ in clear water which may also be related to productivity. This poses a considerable problem for oceanic particle dynamics in that large particles sinking in spring and summer have been considered net scavengers rather than net suppliers of fine particles (Honjo, 1982), in which case one might have expected the spring/summer deep concentration to decrease.

The oceanic particle size spectrum in deep clear water tends to be rather "flat" (McCave, 1983, 1984). This material must arrive partly by disaggregation of larger particles sinking from the surface in order to show this seasonal change, and partly via lateral advection of the low concentration residues of nepheloid layers to supply the aluminosilicate. Large particles falling out of the SNL during summer are mainly aggregates, often including mucus (see SEM results below; cf. Dickson and McCave, 1986) with sinking velocities around 100 $m\,d^{-1}$ or more (Shanks and Trent, 1980; Honjo, 1982; Alldredge and Gotschalk, 1988). Once disaggregated, the particle sinking rates decrease to an order of 100 $m\,a^{-1}$ (aggregates less than 10 μm diameter with density contrasts 0.1–0.5 $g\,cm^{-3}$). Removal of this fine PM is maintained by a combination of particle degradation, reaggregation and scavenging by large sinking patches of marine snow, often dominated by mucus, which have maintained their integrity, gathering particles and sweeping them down to the bed (Honjo, 1982; Hill and Nowell, 1990). Thus it normally has been thought that marine snow is more of a scavenging sink for fine particles than a disaggregating source during periods of high productivity. Nevertheless the congruence with the spatial variation of open ocean mid-water turbidity being higher under higher productivity (Eittreim et al., 1976) suggests the large-particle source effect may be real. Indeed, the same seasonal shift in concentration has recently been described by Sherrell et al. (1998) based on large volume in situ filtration of fine particles from the deep water column off California. They show distinctly higher deep water concentrations below $\sim$1500 m in June (12.1 $mg\,m^{-3}$) than in October and February (7.6 $mg\,m^{-3}$), which also contain higher summer amounts of aluminosilicate (5.1 *vs.* 2.2 $mg\,m^{-3}$). This higher aluminosilicate suggests the possibility of greater lateral advection of bottom-derived sediment in spring and summer. This might be caused by reduced critical erosion stress or even active resuspension due to benthic surface deposit feeders (Thomsen and Flach, 1997). Thus the balance between input from lateral supply and aggregate breakup versus scavenging removal is in favour of input in summer. What we cannot distinguish is whether the deep (2500–3500 m) fine PM has come laterally direct from the slope (this is possible in view of the deep INL seen in Fig. 6, and that shown by Thorpe and White, 1988), or via the

shallower INLs, scavenging and breakup. What does seem highly likely, in view of the high aluminosilicate proportions recorded in the PM at 1200 m by Wollast and Chou (1998), is that there is significant involvement of material resuspended on the slope and moved basinward.

The breakup products of marine snow may be very fine and contain organic matter which is then removed by transformation from particulate to dissolved state (particulate organic matter (POM) → dissolved organic matter (DOM)). If the seasonal shift in concentration is $12\,mg\,m^{-3}$ and if this is 50% POM (~25% POC) the change requires seasonal input and removal of only $3\,mgC\,m^{-3}\,a^{-1}$. This is a relatively small amount compared to the measured deep DOC concentration of $540–640 \pm 12\,mg\,m^{-3}$ (Miller, personal communication; also see Hydes et al., 2001) in which no seasonal variability beyond analytical precision is detected, but it does provide a way of slowly pumping DOC into the deep ocean at a rate that is not out of line with the age of DOC (Druffel et al., 1992). However, in a 2000-m thick water column it amounts to $6\,gC\,m^{-2}\,a^{-1}$ which is large relative to the carbon burial flux of $50–110\,mgC\,m^{-2}\,a^{-1}$. Some of the carbon may also be scavenged and carried down to the bed, providing a winter food source. It should be noted however that Sherrell et al. (1998) found off the California margin that the POC concentration in deep fine PM was similar in summer and autumn/winter (1.31 *vs.* $1.34\,mg\,m^{-3}$), but the aluminosilicate was greater in summer as noted above.

The ~100% increase in deep particle concentration from winter to summer implies a short residence time, of the order of a year or two. This may vary according to which component is considered, but given that lithogenic material is 55% of PM at 1200 m ($PMC = 5.3\,mg\,m^{-3}$)(Wollast and Chou, 1998), it is relevant to the removal timescale of components (such as ^{230}Th) which attach onto surfaces prior to removal.

8. Sources

We need to distinguish between ultimate and immediate sources, particularly for lithogenic material. An immediate source may be the shelf edge, but ultimately this material was mostly emplaced on the outer shelf at the last glacial maximum. Material shed off the shelf is often not derived from modern rivers.

The key to assessing wind-blown material is the data from the uppermost trap farthest off the slope. At OMEX-III (Fig. 1), the 580 m trap flux includes only a trace (i.e., $<0.1\,g\,m^{-2}\,a^{-1}$) of lithogenic material, compared with $13\,g\,m^{-2}\,a^{-1}$ of biogenic (data of Antia et al., 1999), (but Wollast and Chou, 1998 estimate $0.6\,g\,m^{-2}\,a^{-1}$ of lithogenic flux based on Al measurement). Based on Duce et al. (1991), Wollast and Chou suggest an aeolian flux to the surface of $0.1\,g\,m^{-2}\,a^{-1}$ and thus a lateral off-shelf flux of $0.5\,g\,m^{-2}\,a^{-1}$. This trap mooring lies about 150 km from the shelf edge and the material carried off the shelf is rapidly being scavenged into aggregates and sedimented, because the upper trap at OMEX-II (600 m depth, 110 km from shelf) collects ten times as much lithogenic material ($\sim 5\,g\,m^{-2}\,a^{-1}$), presumably transported off the shelf in the surface nepheloid layer.

There is clear evidence of sedimenting material being derived from primary productivity (both organic biomarkers and species compositions of trap samples)(Antia et al., 1999, 2001). However the trapped flux of this material increases with depth in the water column, a trend commonly seen

elsewhere (Biscaye et al., 1988; Honjo and Manganini, 1993), which suggests derivation of part of the flux from resuspended material. For the eventual flux to the bed at a given point it is very difficult to establish precisely the relative importance of the sources. In particular it is hard to distinguish between shelf export of modern supply and resuspension of past supply for lithogenic material, and between primary productivity above the site, shelf export, and resuspension for organic carbon (C_{org}) and skeletal components. So although different sources can be recognised in principle, it is difficult to specify their precise contribution.

As far as the C_{org} is concerned much of the material ultimately is derived from modern primary production, but the preserved carbon on the seabed is older, refractory material with a ^{14}C age of $\sim$3500 a (Hall and McCave, 1998). The terrigenous fraction is ultimately derived from material transported from land by rivers at the last glacial and spread out over the slope at low sea-level. The outer shelf is presently mainly covered in sand (Hamilton et al., 1980), no rivers currently deliver material close to the OMEX site and the regional fluvial loads are small. The nearest is the Loire which supplies 7.8 Mt a^{-1}, while the rivers draining into the English Channel supply less than 5 Mt a^{-1} and the River Severn system about 1.1 Mt a^{-1} (Milliman et al., 1995). These sources are now small and distant whereas at low sea-level the "Great Channel River" of Gibbard (1988), comprising the Rhine-Meuse system and the Thames *plus* all the Channel rivers, would likely have delivered at least 20 Mt a^{-1} to a shelf edge calculated by Lambeck (1995) to be close to Goban Spur (Hall and McCave, 1998). The ultimate source of much of the seabed sediment in the area is thus via fluvial supply at glacial low sea levels.

9. Conclusions

Most of the terrigenous sediment presently being deposited in this area was probably deposited on the outermost shelf and upper slope during the last glacial period by the Great Channel River and Loire. Carbonate is largely from modern biological productivity, as is most of the POC caught in upper and mid-water traps. Preserved carbon however is dominated by refractory old carbon.

The sediment concentration field indicates dynamical processes occurring both in the water column and at the seabed. The water column displays surface, intermediate and bottom nepheloid layers detected by light transmission and scattering. The bottom of the BNLs, and by inference the INLs at the time of their origin, are of high concentration ($\sim$5 g m^{-3} in summer and 1–2 g m^{-3} in winter) and contain aggregated, high settling-velocity (up to 1.6 cm s^{-1}) particles. INLs detected optically are of low concentration and represent residues. The BNL concentrations measured by water bottle filtration at 5–10 m.a.b. are an order of magnitude lower than those measured by in situ pumping at 0.1–0.4 m.a.b. due to dynamical suspension effects which lead to high concentrations of fast settling aggregates close to the bed.

There is a large increase in trapped flux of all components below 1000 m. This is related to topography as there is a broad area of low gradient between 800 and 1400 m depth which both receives material by deposition and provides it to INLs via current- and internal wave-driven resuspension. The main zone of INL ocurrence lies between 1000 and 1500 m. Below 1500 m the slope is steeper and apparently suffers less resuspension. Trapped fluxes, and BNL

and clear-water minimum background concentrations increase in spring and summer in concert with changes in biological productivity. However the unexpected increase in *lithogenic* concentration in the BNL and flux in summer suggests this could be a time of increased sediment resuspension driven by either a more dynamically active water column (less likely) or a critical erosion threshold reduced by benthic macrofaunal activity (more likely) (Thomsen and Flach, 1997).

SEM work on filtered particles suggests fallout of mucus-rich aggregates from the SNL in summer and low background of isolated, mainly terrigenous particles in winter. Sponge fragments in nepheloid layers and clear water indicate resuspension and transport off-slope of mixed aggregates and individual particles in nepheloid layers (intermediate and bottom). The overall higher concentration in BNLs is marked and much material is present as single particles indicating resuspension and breakup.

Large particles measured by snow camera constitute 23% by volume of the total particle population in autumn/winter and 37% during the spring bloom. Although the large particle population in the detaching BNLs is subordinate in volume, we argue that this rapidly sinking particle population initially carried by INLs is responsible for the offshore increase in trapped sediment flux with depth. This trapped flux, taken in conjunction with analysis of suspended material demonstrates that calcium carbonate dissolves profusely in water depths well above the lysocline (over 80%), providing a significant mid-water source of DIC. The trapped fluxes also reveal a pronounced increase in biogenic barium flux with depth, thereby casting doubt on use of barium concentrations in continental margin sediments and under coastal upwelling systems over the slope to infer palaeoproductivity.

The newly observed spring/summer increase and autumn/winter decrease in background fine particle concentration is surprising because it has generally been thought that aggregates from the bloom period acted as net scavengers rather than suppliers of deep PM. However, because there is a significant concentration of lithogenic material involved, some of the increase must have been supplied laterally from the slope. The removal may be accomplished by a combination of particle aggregation and scavenging, remineralisation of carbonate and opal, and POC to DOC conversion. The latter process would have significant implications for carbon budgets. The $\sim$100% seasonal change in clear water minimum PM concentrations implies a residence time for deep particles of 1–2 years depending on composition. These possibilities require and deserve further investigation.

Acknowledgements

This work was supported by the European Union MAST programme (contract no MAS2-CT93-0069 for OMEX project). We are most grateful to the Masters and crews of the many ships involved who made this work possible under sometimes arduous conditions (e.g., winter in the northern Bay of Biscay). We are also most grateful to Dr Amy Bower of Woods Hole Oceanographic Institution for permission to include here preliminary results from floats deployed in ACCE. We thank John Huthnance and especially the reviewers of this paper, Pierre Biscaye, Wilf Gardner and André Monaco whose critiques have improved it considerably. Cambridge Earth Sciences publication ES-5465.

References

Alldredge, A.L., Gotschalk, C., 1988. In situ settling behaviour of marine snow. Limnology and Oceanography 33, 339–351.

Allen, J.R.L., 1971. A theoretical and experimental study of climbing-ripple cross-lamination, with a field application to the Uppsala esker. Geografiska Annaler 53A, 157–187.

Anderson, R.F., Rowe, G.T., Kemp, P.F., Trumbore, S., Biscaye, P.E., 1994. Carbon budget for the mid-slope depocenter of the Middle Atlantic Bight. Deep-Sea Research II 41, 669–703.

Antia, A.N., Maaßen, J., Herman, P., Voß, M., Scholten, J., Groom, S., Miller, P., 2001. Spatial and temporal variability of particle flux at the N.W. European continental margin. Deep-Sea Research II 48, 3083–3106.

Antia, A.N., von Bodungen, B., Peinert, R., 1999. Particle flux across the mid-European continental margin. Deep-Sea Research I 46, 1999–2024.

Baker, E.T., Hickey, B.M., 1986. Contemporary sedimentation processes in and around an active West Coast submarine canyon. Marine Geology 71, 15–35.

Baker, E.T., Lavelle, J.W., 1984. The effects of particle size on the light attenuation coefficient of natural suspensions. Journal of Geophysical Research 89, 8197–8203.

Baker, E.T., Milburn, H.B., Tennant, D.A., 1988. Field assessment of sediment trap efficiency under varying flow conditions. Journal of Marine Research 46, 573–592.

Bartz, R., Zaneveld, J.R.V., Pak, H., 1978. A transmissometer for profiling and moored observations in water. Proceedings of the Society of Photo-Optical Instrumentation Engineers 160, 102–108.

Belderson, R.H., Pingree, R.D., Griffiths, D.K., 1986. Low sea-level origin of Celtic Sea sand-banks—evidence from numerical modelling of M2 tidal streams. Marine Geology 73, 99–108.

Biscaye, P.E., Anderson, R.F., Deck, B.L., 1988. Fluxes of particles and constituents to the eastern United states continental slope and rise: SEEP-I. Continental Shelf Research 8, 855–904.

Biscaye, P.E, Eittreim, S.L, 1977. Suspended particulate loads and transports in the nepheloid layer of the abyssal Atlantic Ocean. Marine Geology 23, 155–172.

Biscaye, P.E., Flagg, C.N., Falkowski, P.G., 1994. The shelf edge exchange processes experiment, SEEP-II an introduction to hypotheses, results and conclusions. Deep-Sea Research II 41, 231–252.

Bishop, J.K.B., 1986. The correction and suspended particulate matter calibration of SeaTech transmissometer data. Deep-Sea Research 33, 121–134.

Bishop, J.K.B., 1988. The barite-opal-organic carbon association in oceanic particulate matter. Nature 332, 341–343.

Bishop, J.K.B., Collier, R.W., Ketten, D.R., Edmond, J.M., 1980. The chemistry, biology and vertical flux of particulate matter from the upper 1500 m of the Panama Basin. Deep-Sea Research 27, 615–640.

Blake, J.A., Diaz, R.J., 1994. Input, accumulation and cycling of materials on the continental slope off Cape Hatteras: An introduction. Deep-Sea Research II 41, 707–711.

Brewer, P.G., Spencer, D.W., Biscaye, P.E., Hanley, A., Sachs, P.L., Smith, C.L., Kadar, S., Fredericks, J., 1976. The distribution of particulate matter in the Atlantic. Earth and Planetary Science Letters 32, 393–402.

Chatwin, P.G., 1996. Near-bed flows and sediment movement on the continental slope. Ph.D. thesis, Institute of Marine Studies, University of Plymouth, UK.

Churchill, J.H., Biscaye, P.E., Aikman, F., 1988. The character and motion of suspended particulate matter over the shelf edge and upper slope off Cape Cod. Continental Shelf Research 8, 789–809.

Dehairs, F., Fagel, N., Antia, A.N., Peinert, R., Elskens, M., Goeyens, L., 2000. Export production in the Bay of Biscay as estimated from barium-barite in settling material: a comparison with new production. Deep-Sea Research I 47, 167–186.

Dickson, R.R., Gould, W.J., Gurbutt, P.A., Killworth, P.D., 1982. A seasonal signal in ocean currents to abyssal depths. Nature 295, 193–198.

Dickson, R.R., Gould, W.J., Muller, T.J., Maillard, C., 1985. Estimates of the mean circulation in the deep (> 2000 m) layer of the eastern North Atlantic. Progress in Oceanography 10, 813–819.

Dickson, R.R., McCave, I.N., 1986. Nepheloid layers on the continental slope west of Porcupine Bank. Deep-Sea Research 33, 791–818.

Drake, D.E., 1971. Suspended sediment and thermal stratification in Santa Barbara Channel, California. Deep-Sea Research 18, 763–769.

Drake, D.E., 1974. Distribution and transport of suspended particulate matter in submarine canyons off southern California. In: Gibbs, R.J. (Ed.), Suspended Solids in Water. Plenum Press, New York, pp. 133–153.

Druffel, E.R.M., Williams, P.M., Bauer, J.E., Ertel, J.R., 1992. Cycling of dissolved and particulate organic matter in the open ocean. Journal of Geophysical Research 97, 15 639–15 659.

Duce, R.A., Liss, P.S., Merrill, J.T., Atlas, E.L., Buat-Ménard, P., Hicks, B.B., Miller, J.M., Prospero, J.M., Arimoto, R., Church, T.M., Ellis, W., Galloway, J.N., Hansen, L., Jickells, T.D., Knap, A.H., Reinhardt, K.H., Schneider, B., Soudine, A., Tokos, J.J., Tsunogai, S., Wollast, R., Shou, M., 1991. The atmospheric input of trace species to the world oceans. Global Biogeochemical Cycles 5, 193–259.

Durrieu de Madron, X., Etcheber, H., Froidefond, J., Godet, C., Jouanneau, J.M., Laborde, P., Nyffeler, F., Ruch, P., Urrutia, J., Valencia, V., Weber, O., 1993. North East Atlantic continental margin (ECOFER) suspended material and primary production. Annales de L'Institut Oceanographique 69, 155–159.

Durrieu de Madron, X., Nyffeler, F., Godet, C.H., 1990. Hydrographic structure and nepheloid spatial distribution in the Gulf of Lions continental margin. Continental Shelf Research 10, 915–929.

Dymond, J., Suess, E., Lyle, M., 1992. Barium in deep-sea sediment: a geochemical proxy for paleoproductivity. Paleoceanography 7, 163–181.

Eittreim, S., Ewing, M., 1974. Turbidity distribution in the deep waters of the western Atlantic trough. In: Gibbs, R.J. (Ed.), Suspended Solids in Water. Plenum Press, New York, pp. 213–225.

Eittreim, S., Thorndike, E.M., Sullivan, L., 1976. Turbidity distribution in the Atlantic Ocean. Deep-Sea Research 23, 1115–1127.

Francois, R., Honjo, S., Manganini, S.J., Ravizza, G.E., 1995. Biogenic barium fluxes to the deep sea: implications for paleoproductivity reconstruction. Global Biogeochemical Cycles 9, 289–303.

Gardner, W.D., 1985. The effect of tilt on sediment trap efficiency. Deep-Sea Research 32, 349–361.

Gardner, W.D, 1989a. Baltimore Canyon as a modern conduit of sediment to the deep sea. Deep-Sea Research 36, 323–358.

Gardner, W.D., 1989b. Periodic resuspension in Baltimore Canyon by focussing of internal waves. Journal of Geophysical Research 94, 18 185–18 194.

Gardner, W.D., Biscaye, P.E., Richardson, M.J., 1997. A sediment trap experiment in Vema Channel to evaluate the effect of horizontal particle fluxes on measured vertical fluxes. Journal of Marine Research 55, 995–1028.

Gardner, W.D., Biscaye, P.E., Zaneveld, J.R.V., Richardson, M.J., 1985. Calibration and composition of the LDGO nephelometer and the OSU transmissometer on the Nova Scotian Rise. Marine Geology 66, 323–344.

Gibbard, P.L., 1988. The history of the great northwest European rivers during the past three million years. Philosophical Transactions of the Royal Society of London B318, 559–602.

Graf, G., Gerlach, S.A., Linke, P., Queisser, W., Scheltz, A., Thomsen, L., Witte, U., 1995. Benthic-Pelagic coupling in the Greenland-Norwegian Sea and its effects on the geological record. Geologische Rundschau 84, 49–58.

Gross, T.F., Nowell, A.R.M., 1990. Turbulent suspension of sediments in the deep sea. Philosophical Transactions of the Royal Society of London A 331, 167–181.

Gross, T.F., Williams, A.J., 1991. Characterisation of deep sea storms. Marine Geology 99, 281–301.

Hall, I.R, McCave, I.N., 1998. Glacial-interglacial variation in organic carbon burial on the slope of the N.W. European Continental Margin (48°–50°N) Progress in Oceanography 42, 37–60.

Hamilton, D., Sommerville, J.H., Stanford, P.N., 1980. Bottom currents and shelf sediments, southwest of Britain. Sedimentary Geology 26, 115–138.

Harvey, J., 1982. θ–S relationships and water masses in the eastern North Atlantic. Deep-Sea Research 29, 1021–1033.

Hill, P.S., Nowell, A.R.M., 1990. The potential role of large, fast-sinking particles in clearing nepheloid layers. Philosophical Transactions of the Royal Society of London A331, 103–117.

Honjo, S., 1982. Seasonality and interaction of biogenic and lithogenic particulate flux at the Panama Basin. Science 218, 883–884.

Honjo, S., 1996. Fluxes of particles to the interior of the open oceans. In: Ittekkot, V., Schäfer, P., Honjo, S., Hepeteris, P.J. (Eds.), Particle Flux in the Ocean. Wiley, New York, pp. 91–154.

Honjo, S., Manganini, S.J., 1993. Annual biogenic particle fluxes to the interior of the North-Atlantic Ocean studies at 34°N 21°W. Deep-Sea Research II 40, 587–607.

Huthnance, J.M., 1995. Circulation, exchange and water masses at the ocean margin: the role of physical processes at the shelf edge. Progress in Oceanography 35, 353–431.

Hydes, D.J., Le Gall, A.C., Miller, A.E.J., Brockmann, U., Raabe, T., Holley, S., Alvarez-Salgado, X., Antia, A., Balzer, W., Chou, L., Elskens, M., Helder, W., Joint, I., Orren, M., 2001. Supply and demand of nutrients and dissolved organic matter at and across the NW European shelf break in relation to hydrography and biogeochemical activity. Deep-Sea Research II 48, 3023–3047.

Johnson, M.A., Kenyon, N.H., Belderson, R.H., Stride, A.H., 1982. Sand transport. In: Stride, A.H. (Ed.), Offshore Tidal Sands, Processes and Deposits. Chapman & Hall, London, pp. 58–94.

Joint, I., Wollast, R., Chou, L., Batten, S., Elskens, M., Edwards, E., Hirst, A., Burkill, P., Groom, S., Gibb, S., Miller, A., Hydes, D., Dehairs, F., Antia, A., Barlow, R., Rees, A., Pomroy, A., Brockmann, U., Cummings, D., Lampitt, R., Loijens, M., Mantoura, F., Miller, P., Raabe, T., Salgado, X., Stelfox, C., Woolfenden, J., 2001. Pelagic production at the Celtic Sea shelf break. Deep-Sea Research II 48, 3049–3081.

Lambeck, K., 1995. Late Devensian and Holocene shorelines of the British Isles and North Sea from models of glacio-hydro-isostatic rebound. Journal of the Geological Society, London 152, 437–448.

Lampitt, R.S., Hillier, W.R., Challenor, P.G., 1993a. Seasonal and diel variation in the open ocean concentration of marine snow aggregates. Nature 362, 737–739.

Lampitt, R.S., Wisher, K.F., Turley, C.M., Angel, M.V., 1993b. Marine snow studies in the Northeast Atlantic: distribution, composition and role as a food source for migrating plankton. Marine Biology 116, 689–702.

Martin, J.H., Knauer, J.A., Karl, D.M., Broenkow, W.W., 1987. VERTEX: carbon cycling in the Northeast Pacific. Deep-Sea Research 34, 267–285.

Martin, J.H., Whitfield, M., 1983. The significance of the river input of chemical elements to the ocean. In: Wong, C.S., Boyle, E.A., Burton, J.D. (Eds.), Trace Metals in Sea Water. Plenum Press, New York, pp. 265–296.

McCartney, M.S., 1992. Recirculating components to the deep boundary current of the Northern North Atlantic. Progress in Oceanography 29, 283–383.

McCave, I.N., 1975. Vertical flux of particles in the ocean. Deep-Sea Research 22, 491–502.

McCave, I.N., 1983. Particulate size spectra, behaviour, and origin of nepheloid layers over the Nova Scotian Continental Rise. Journal of Geophysical Research 88, 7647–7666.

McCave, I.N., 1984. Size spectra and aggregation of suspended particles in the deep ocean. Deep-Sea Research 31, 329–352.

McCave, I.N, 1985. Properties of suspended sediment over the HEBBLE area on the Nova Scotian continental rise. Marine Geology 66, 169–188.

McCave, I.N., 1986. Local and global aspects of the bottom nepheloid layers in the world ocean. Netherlands Journal of Sea Research 20, 167–181.

Milliman, J.D., 1993. Production and accumulation of calcium carbonate in the ocean: budget of non-steady state. Global Biogeochemical Cycles 7, 927–957.

Milliman, J.D., Rutkowski, C., Meybeck, M., 1995. River discharge to the sea: a Global River Index (GLORI), LOICZ Reports and Studies, LOICZ Core Project Office, Texel, The Netherlands.

Monaco, A., Biscaye, P., Soyer, J., Pocklington, R., Heussner, S., 1990. Particle fluxes and ecosystem response on a continental margin: the 1985–1988 Mediterranean Ecomarge experiment. Continental Shelf Research 10, 809–839.

Moody, J.A., Butman, B., Bothner, M.H., 1986. Near-bottom suspended matter concentrations during storms. Continental Shelf Research 7, 609–628.

Newton, P.P., Lampitt, R.S., Jickells, T.D., King, P., Boutle, C., 1994. Temporal and spatial variability of biogenic particle fluxes during the JGOFS northeast Atlantic process studies at 47°N, 20°W. Deep-Sea Research I 41, 1617–1642.

Pingree, R.D., Le Cann, B., 1989. Celtic and Armorican slope and shelf residual currents. Progress in Oceanography 23, 303–339.

Pingree, R.D., Sinha, B., Griffiths, C.R., 1999. Seasonality of the European slope current (Goban Spur) and ocean margin exchange. Continental Shelf Research 19, 929–975.

Richardson, M.J., 1987. Particle size, light scattering and composition of suspended particulate matter in the North Atlantic. Deep-Sea Research 34, 1301–1329.

Richardson, M.J., Hollister, C.D., 1987. Compositional changes in particulate matter on the Iceland Rise, through the water column, and at the seafloor. Journal of Marine Research 45, 175–200.

Ritzrau, W., Thomsen, L., 1997. Spatial distribution of particle composition and microbial activity in the benthic bounday layer (BBL) of the North East Water Polyna. Journal of Marine Systems 10, 415–428.

Ruch, P., Mirmand, M., Jouanneau, J.M., Latouche, C., 1993. Sediment budget and transfer of suspended sediment from the Gironde Estuary to Cap Ferret Canyon. Marine Geology 111, 109–119.

Shanks, A.L., Trent, J.D., 1980. Marine snow: sinking rates and potential role in vertical flux. Deep-Sea Research 27, 137–143.

Sherrell, R.M., Field, M.P., Gao, Y., 1998. Temporal variability of suspended mass and composition in the Northeast Pacific water column: relationship to sinking flux and lateral advection. Deep-Sea Research Part II 45, 733–761.

Spinrad, R.W., Zaneveld, J.R.V., Kitchen, J.C., 1983. A study of the optical characteristics of the suspended particles in the benthic nepheloid layer of the Scotian Rise. Journal of Geophysical Research 88, 7641–7645.

Sternberg, R.W., Berhane, I., Ogston, A.S., 1999. Measurement of size and settling velocity of suspended aggregates on the northern California continental shelf. Marine Geology 154, 43–53.

Thomsen, L., Flach, E., 1997. Mesocosm observations of fluxes of particulate matter within the benthic boundary layer. Journal of Sea Research 37, 67–79.

Thomsen, L., Graf, G., 1995. Benthic boundary layer characteristics of the continental margin of the western Barents Sea. Oceanologica Acta 17, 597–607.

Thomsen, L., Graf, G., Martens, V., Steen, E., 1994. An instrument for sampling water from the benthic boundary layer. Continental Shelf Research 14, 87–882.

Thomsen, L., McCave, I.N., 2000. Aggregation processes in the benthic boundary layer at the Celtic Sea continental margin. Deep-Sea Research I 47, 1389–1404.

Thomsen, L., Ritzrau, W., 1996. Aggregate studies in the benthic boundary layer at a continental margin. Journal of Sea Research 36, 143–146.

Thomsen, L., van Weering, T.C.E., 1998. Spatial and temporal variability of particulate matter in the benthic boundary layer at the NW European Continental Margin (Goban Spur). Progress in Oceanography 42, 61–76.

Thorpe, S.A, White, M., 1988. An intermediate nepheloid layer. Deep-Sea Research 35, 1655–1671.

Vangriesheim, A., Khripounoff, A., 1991. Near bottom particle concentration and flux - temporal variations observed with sediment traps and nephelometer on the Meriadzeck Terrace, Bay of Biscay. Progress in Oceanography 24, 103–116.

Walsh, J.J., Biscaye, P.E., Csanady, G.T., 1988. The 1983–1984 shelf edge exchange processes (SEEP)-1 experiment: hypotheses and highlights. Continental Shelf Research 8, 435–457.

Walsh, J.J., Rowe, G.T., Ivenson, R.L., McRoy, C.P., 1981. Biological export of shelf carbon: a neglected sink of the global CO_2 cycle. Nature 291, 196–201.

van Weering, T.C.E., Hall, I.R., McCave, I.N., De Stigter, H., Thomsen, L., 1998. Recent sediments, sediment accumulation and carbon burial at Goban Spur. NW European Continental Margin (47–50N). Progress in Oceanography 42, 5–35.

von Bodungen, B., Wunsch, M., Fürdere, H., 1991. Sampling and analysis of suspended and sinking particles in the North Atlantic. Geophysical Monograph 63, 47–56.

Wollast, R., Chou, L., 1998. Distribution and fluxes of calcium carbonate along the continental margin in the Gulf of Biscay. Aquatic Geochemistry 4, 369–393.

Zaneveld, J.R.V., 1974. Variation of optical sea properties with depth. In: Optics of the Sea. Interface and in-Water Transmission and Imaging, NATO Lecture Series, Vol. 61, pp. 2.3-1–2.3-22.